國立臺灣大學生命科學院漁業科學研究所

碩士論文

Institute of Fisheries Science
College of Life Science
National Taiwan University

Master Thesis

胰島素樣生長因子結合蛋白在鯖鰭魚離子調控之角色

The role of insulin-like growth factor binding proteins in ion regulation of Indian medaka (*Oryzias melastigma*)

唐玉欣
Yu-Hsin Tang
指導教授：黃鵬鵬 博士
王永松 博士
Advisor: Pung-Pung Hwang, Ph.D.
Yung-Song Wang, Ph.D.

中華民國 109 年 7 月

July, 2020

doi:10.6342/NTU202002011

謝辭

在碩士班的這兩年，深深感謝這些日子以來參與我研究生活的大家，謝謝各位的幫忙以及支持，才讓我可以順利拿到碩士學位。首先，很感謝我的指導教授黃鵬鵬老師及王永松老師對我用心的指導與幫助。在和黃老師討論時，總會感受到老師的熱情與活力，也刺激著我以不同的角度去思考。也謝謝王老師在我報進度時，給予我大大的鼓勵，讓我更有勇氣面對挫折。兩位老師對於研究的熱忱及態度，都是我值得學習的目標。同時也謝謝碩士論文口試委員中研院細生所曾庸哲老師及台大生科系周銘翊老師在論文上給予我寶貴的指導及建議，讓我能順利完成這本論文。

在實驗上，感謝 LAA 哥在知識上的教導給了我很多解決問題的方法，及不辭勞苦幫我看論文不足之處，也要感謝天天一直用心地教我實驗，才能傳承學姊厲害的 *in situ* 技術，董姐幫我處理繁雜的行政事務，芝萱和學姐們辛苦打理魚房，小丸子 journal club 的知識交流及卷餅，Amy 姐辛苦的電生理以及接下行政一職重任，慧文和若冬學姊教我的基本分生技術，紹葳和尚武在實驗上幫忙我的大小事及技術指導，小莊、邱翎幫我處理口試前事務，讓我能專心準備口試。小胖教我用 AAS，語婕幫我餵胖孔雀魚，也謝謝威行、柏鈞、雅婷為實驗室日常帶來許多活潑。同時也感謝周老師在碩一訓練我報告的技巧、以及思考的邏輯。謝謝和曾老師一起的聯合 meeting，讓我更進步。感謝阿淳、美如、麻吉、敏真、寶龍、孟偉和怡安對我平時的關心和照顧，也要謝謝 Peggy 和杜杜教我使用儀器和處理儀器問題，以及感謝無數可愛 medaka 的犧牲奉獻，讓我的實驗順順利利！同時也感謝漁科及海研的夥伴汶諭、家敏、思維、資蓉讓我的研究生活充滿樂趣，恰克的包容和幫我美化可愛的蛋～

最後在研究的路上，特別謝謝我的家人對我無條件的支持，總是給我鼓勵，讓我沒有後顧之憂地完成學業及寶貝嘟嘟在我低潮時的陪伴。真心感謝這些陪伴在我身邊的人們，謝謝你們的包容和傾聽，謝謝！

doi:10.6342/NTU202002011

中文摘要

魚類鰓或胚胎表皮上的離子細胞是群負責滲透壓調節的特化細胞。目前已知胰島素樣生長因子 (IGF) 可以調控離子運輸蛋白的表現及離子細胞型態，以適應高滲透壓的環境。最近的研究發現，IGF 結合蛋白(IGFBP)家族中，斑馬魚 *igfbp5a* 在胚胎離子細胞中對於鈣離子的恆定扮演重要的角色。大部分對於硬骨魚 IGFBP 家族的研究集中在面對各種壓力下的生長反應，然而，很少去探究面對鹽度刺激的反應。因此，在本篇研究中，我們利用廣鹽性魚類，印度鯖鰶魚做為調查 IGFBP 家族是否參與離子調控的模式動物。在印度鯖鰶魚中，發現有 11 個 IGFBP 家族的基因。其中，10 型於鰓有表現(*igfb1a*, *-1b*, *-2a*, *-2b*, *-3b*, *-4*, *-5a*, *-5b*, *-6a* 和 *-6b*)，但只有 *igfbp5a* 主要表現在鰓中。將成魚轉移到海水後，大部分 *igfbp* 基因在鰓的表現量皆顯著下降。原位雜交及免疫組織化學染色的結果顯示，*igfbp5a* 表現在標定離子細胞的鈉鉀離子幫浦蛋白質旁邊的較小細胞中。雙標記原位雜交顯示出 *igfbp5a* 與上皮鈣離子通道（*trpv6*/*ecac*）表現位置相同，該通道是 ECaC 離子細胞的標誌，負責在淡水中吸收鈣離子。有趣的是，當胚胎適應在低鈣離子濃度環境時，表達 *igfbp5a* 與 *trpv6* 的細胞數量顯著增加。另外，我們還發現，當阻斷 IGF 訊息傳遞後，在低鈣環境下 *trpv6* 細胞數量的增加與鈣吸收的能力皆受到明顯的抑制。這些實驗結果顯示，印度鯖鰶魚在低鈣環境時，可能通過 *igfbp5a* 參與 IGF 訊息傳遞的機制，不但增加 *trpv6* 細胞的數量，同時也增加單細胞中鈣離子吸收的能力。

關鍵字：胰島素樣生長因子結合蛋白、離子調節、鈣離子恆定、離子細胞、上皮鈣離子通道、印度鯖鰶魚

doi:10.6342/NTU202002011

Abstract

Ionocytes in fish gills and embryonic skin are specialized cells responsible for osmoregulation. Insulin-like growth factor (IGF) signaling has been known to regulate the expression of transporters and the morphology of ionocytes for hyperosmotic adaptation. Recently, one of IGF binding protein (IGFBP), *igfbp5a*, has been identified in embryonic ionocytes to play a role in calcium homeostasis in zebrafish. Studies on teleost IGFBPs were focused on how they mediate growth responses to stressors, while few studies investigated the responses after salinity challenge. In the present study, we aimed to investigate whether IGFBPs participate in ion regulation in a euryhaline species, Indian medaka (*Oryzias melastigma*). We found totally 11 IGFBP genes in Indian medaka. Among them, ten of IGFBP members (*igfb1a*, *-1b*, *-2a*, *-2b*, *-3b*, *-4*, *-5a*, *-5b*, *-6a* and *-6b*) are expressed in the gills, but only *igfbp5a* is dominantly expressed. Most of branchial *igfbps* expression were down-regulated after seawater exposure. *In situ* hybridization and immunocytochemistry showed that *igfbp5a* was expressed in the smaller adjacent cells next to Na^+-K^+-ATPase-labeled ionocytes. Besides, double-labeled ISH showed that the expression of *igfbp5a* was co-localize with the epithelial Ca^{2+} channel (*trpv6*/*ecac*) which is a marker of ECaC ionocyte for Ca^{2+} absorption in the freshwater. Interestingly, the number of *igfbp5a* and *trpv6* expressing cells increased when acclimated to low [Ca^{2+}] water. In addition, blockage of IGF signaling not only inhibits the increment of *trpv6* expressing cells, but also impaired the ability of Ca^{2+} absorption of the ionocytes after low [Ca^{2+}] acclimation. These results suggested, through *igfbp5a*, IGF signaling involved in the Ca^{2+} absorption mechanism by increase the Ca^{2+} uptake and *trpv6* expressing cells under low [Ca^{2+}] water in the Indian medaka.

doi:10.6342/NTU202002011

Keywords: Insulin-like growth factor binding protein, ion regulation, Ca^{2+} homeostasis, ionocyte, epithelial Ca^{2+} channel, Indian medaka

doi:10.6342/NTU202002011

Contents

doi:10.6342/NTU202002011

doi:10.6342/NTU202002011

doi:10.6342/NTU202002011

List of tables

doi:10.6342/NTU202002011

List of figures

doi:10.6342/NTU202002011

1. Introduction

1.1 Fish ion regulation

Osmotic homeostasis is essential for physiological processes in fish. To adapt the oscillation of osmotic gradients in aquatic environments, fish have developed iono/osmoregulation mechanisms by ionocytes (also known as chloride cells or mitochondrion-rich cells), which are specialized cells mainly on adult gills or embryonic skin in fish, instead of kidneys in mammals (Hwang et al., 2011). Ionocytes express specific ion-transporting proteins (transporters or enzymes) to transport ions in the apical and basolateral membranes, which are critical for maintain the ionic compositions of body fluids (Hirose et al., 2003; Evans et al., 2005; Hwang and Lee, 2007).

Euryhaline fishes are able to tolerate within a wide range of salinities because of their advantageous osmoregulatory abilities, they can maintain the osmolarity (300–350 mOsm) of their extracellular body fluid (Reinecke, 2010). It is contributed to their ionocytes which have specific types and distinct ion-transporting proteins for different functions in FW and SW respectively. Among the ion-transporting proteins, Na^+/K^+-ATPase (NKA) is a key enzyme provide the driving force for ion transport by creating electronic and ionic gradients across the plasma membrane, and thus providing the driving force for ion transport in both FW and SW (Skou and Esmann, 1992). FW-type ionocytes or SW-type ionocytes can transform into other types of ionocytes, and thus changing the functions. *In vivo* study indicated that when the tilapia embryo transferred from FW to SW for 96 hours, the pre-exiting FW ionocytes transformed into the SW ones. Similar transformation is also proposed to occur in medaka. (Inokuchi et al., 2017; Shen et al., 2011; Hiroi et al., 1999; Hsu et al., 2014). When fishes live in FW, ionocytes are responsible for ion uptake to compensate for the passive loss of ions. According to

doi:10.6342/NTU202002011

different FW-acclimated teleosts, the mechanisms for ion uptake in ionocytes are variable (Hwang and Lin, 2013). There are three distinct FW-type ionocytes in Japanese medaka (*Oryzias latipes*). The presence of Na^+/Cl^- cotransporter (NCC) is identified as NCC cell, it localizes in the apical membrane. Because of the presence of Na^+/H^+ exchanger 3 (NHE3) in the apical membrane of the second type, it is classified as NHE cell. Besides, the third FW-type ionocyte is characterized as ECaC cell with the presence of epithelial calcium channel (ECaC/Trpv6) in the apical membrane (Hiroi et al., 2008; Inokuchi et al., 2008; Hsu et al., 2014). By contrast, ionocytes excrete excess ions which contributed to maintain the stability of the plasma osmotic pressure in SW. The currently accepted model proposes that one distinct SW-type ionocyte could active ion secretion. It is mediated by $Na^+/K^+/2Cl^-$ cotransporter 1a (NKCC1a) in the basolateral membrane, and the cystic fibrosis transmembrane conductance regulator (CFTR) in the apical membrane (Hwang and Lin, 2013). This ionocyte is referred to as SW cell. In addition, SW-type ionocytes are companied frequently with accessory cells (ACs) that express less basolateral NKA. They can form multicellular complex to drive Na^+ transport through the leaky junction (Hwang and Hirano, 1985). As a result, these ionocytes have been considered to be responsible for osmoregulation in fishes.

1.2 Growth hormone (GH) and insulin-like growth factor 1 (IGF1) axis in osmoregulation

Several endocrine systems play roles in osmotic regulation in euryhaline teleost. For example, the growth hormone (GH)/ insulin-like growth 1 (IGF1) axis has been studied to influence on ionoregulatory functions in fishes transferred from FW to SW (McCormick et al., 2013). The GH and IGF1 levels significantly increase in different teleosts raised in saline water, include: *I. punctatus* (Tang et al., 2001), *O. mykiss*

doi:10.6342/NTU202002011

(Shepherd et al., 2005; Liebert and Schreck, 2006) and *G. przewalskii* (Cao et al., 2009). The osmoregulatory actions of GH may mediated by multiple pathways. GH released from the anterior pituitary can stimulate synthesis of endocrine IGF1 in the liver or paracrine/autocrine IGF1 in the gills via GH receptor (GHR). Global or local secretion of IGF1 may interact with the type 1 IGF receptor (IGF1R) and exerts its ionic regulatory effects in the circulation and target tissue (Reinecke, 2010).

GH is a polypeptide hormone with a role in osmotic acclimation (Mancera and McCormick, 1998) as well as growth and energy metabolism in fish (Bjornsson, 1997). Recent studies have been demonstrated that injections with GH increased hypoosmoregulatory ability and salinity tolerance in a variety of salmonid species, it seems to enhance branchial NKA activity, the mRNA expression of *NKCC*, chloride cell size and density (Mancera and McCormick, 1998). Similar effects have been indicated in other species, include two tilapias, *O. niloticus* and *O. mossambicus* (Shepherd et al., 1997) *killifish* (Mancera and McCormick, 1998), and *S. sarba* (Deane et al., 1999). In addition, some *in vivo* and *in vitro* researches have suggested that IGF1 plays a physiological role as well as GH in osmoregulation (Seidelin and Madsen, 1999; Seidelin et al., 1999).

IGF1 is evolutionarily ancient polypeptide and its structure is related to insulin. Insulin primarily plays a key role in an endocrine action to regulate metabolism, whereas IGF1 can have a variety of roles as endocrine, paracrine and autocrine factors that promote the growth, differentiation, proliferation and survival in vertebrates (Duan and Plisetskaya, 1993; Shamblott and Chen, 1992). In addition to growth, IGF1 has also been associated with fish development, metabolism, reproduction and osmoregulation in seawater (Reinecke et al., 2005). These and other biological functions of IGF1 are mediated by binding to and activating the IGF1R, a receptor tyrosine kinase that is

doi:10.6342/NTU202002011

structurally associated with the insulin receptor in several tissues (Reinecke et al., 2005), and regulating the proliferation and differentiation pathway for the development of salt secreting chloride cells in the gills. When treatment with both GH and IGF1, fish have higher salinity tolerance than either hormone alone (Mancera and McCormick, 1998). Consequently, regardless of the GH, IGF1 can participate in the ion regulation to promote salinity tolerance.

1.3 Insulin-like growth factor binding protein (IGFBP)

Most IGF can interact with a member of a cognate proteins family termed as IGF binding proteins (IGFBPs) family in the bloodstream. These IGFBPs are capable of binding IGFs with equal or greater affinity than the affinity between IGF1 and its receptor. (Firth and Baxter, 2002). Therefore, IGFBPs play a key position to regulate IGF signaling globally. When IGF binds to IGFBP, it can increase the half-life in the circulation and prevent the potential binding to the insulin receptor (Firth and Baxter, 2002; Taguchi and White, 2008). In addition to these endocrine roles, IGFBPs have been shown to modulate IGF signaling locally in target tissues (Duan et al., 2010). However, IGFBP family of teleost fishes remains poorly understood compared to the mammalian system.

1.3.1 The IGFBP family and structural feature

The IGFBP family is highly conserved and evolutionarily ancient in vertebrates (Daza, et al., 2011; Duan and Xu, 2005; Upton, et al., 1993). In mammals, IGFBPS have been designated to six types, including IGFBP1 to IGFBP6. However, some teleost may retain duplicated copies (paralogs) for more Igfbp subtypes or occasionally lack one or more of the types (Duan and Larhammar, 2011; Macqueen, et al., 2013). It is attributable to successive rounds of whole genome duplications in teleosts (Van, et al., 2017;

doi:10.6342/NTU202002011

Macqueen and Johnston, 2014). IGFBPs contain approximately 200–300 amino acids and a conserved structure across species. This structure consists of a highly cysteine-rich N-terminal domain, C-terminal domain and a variable linker domain between them. These domains participate in forming the IGF-binding site. Besides, the unstructured central linker domain not only serve to link the N- and C-terminal domains together but also provides a location for functional motifs binding, including the components of the extracellular matrix, cell surface proteoglycans, proteolytic cleavage sites, heparin binding sites, post-translational modification sites, etc. (Firth and Baxter, 2002; Jones and Clemmons, 1995). Therefore, function of different IGFBPs determined by unique composition of functional motifs among them.

1.3.2 IGFBP biological action

Although all IGFBP family members bind circulating IGF to regulate growth (Denley et al., 2005), they also have individual roles to regulate the hormones delivery and interaction with IGF1R locally (Duan et al., 2010). Recent studies have proposed that local IGFBPs could act both positively and negatively under various conditions in target tissues (Duan et al., 2010). The diverse functions are determined by the level of competition between IGFBPs and IGF1R for IGF (Siwanowicz et al., 2005). IGFBPs generally bind IGFs with equal or higher affinity than the IGF1R and thus can inhibit IGF signaling (Baxter, 2014; Jones and Clemmons, 1995). In contrast, some IGFBPs have been shown to potentiate IGF signaling with IGFBPs proteases. These proteases can cleavage fragments responsible for binding IGFs, and leads to more IGFs available for IGF1R binding (Imai et al., 1997). Also, when IGFBP binds to the target cell's surface proteoglycans or extracellular matrix components, it can increase a concentration of local IGF being released to the IGF1R at target sites (Imai et al., 1997; Oxvig, 2015).

doi:10.6342/NTU202002011

1.3.3 IGFBPs as regulators of ionic homeostasis

Previous studies on teleost Igfbps have primarily focused on how they mediate growth responses to stressors about fasting, temperature, and hypoxia, etc. Only few studies have investigated IGFBP responses to ionoregulatory challenges (Dai et al., 2014; Reindl and Sheridan, 2012; Taniyama et al., 2016). However, there is also emerging evidences about ionoregulatory role of IGFBPs in ionic homeostasis.

In zebrafish, *igfbp5* paralogues (*igfbp5a* and *igfbp5b*) were expressed in the gill prominently and even higher than in the liver (Zhou et al., 2008, Dai et al., 2010). Besides, *igfbp5a* expressing cells were localized to a sub-population of zebrafish ionocytes identified as NKA-rich (NaR) cells responsible for Ca^{2+} uptake via ECaC channels. *Igfbp5a* acting to regulate IGF signaling for NaR cells' proliferation induced by low environmental [Ca^{2+}] and plays an essential role in Ca^{2+} homeostasis (Dai et al., 2010). In salmon, *igfbp4*, *igfpbp5*, and *igfbp6* were found to have higher expression in gills than other surveyed tissues (Macqueen et al., 2013). When salmon migrated to seawater in the spring, *igfbp4* and *igfbp6* expression exhibited an increment, but *igfbp5a*, *−5b1* and*−5b2* were all reduced following SW exposure (Breves et al., 2017). Recent study found strong evidence for divergence of *igfbp2a* and *igfbp5a* between marine and freshwater stickleback ecotypes. Among them, *igfbp5a* was most highly expressed in stickleback gill with RNA sequence analyses on transcriptomes from many tissues (Pellissier et al., 2018). To sum up, this evidence suggests that IGFBPs may potentially play roles in salinity tolerance or ionic homeostasis. However, the detailed mechanisms are still unclear. It is necessary to elucidate whether IGFBPs involved in ionic regulatory mechanisms in teleost.

doi:10.6342/NTU202002011

1.4 Indian medaka as a model to study fish ion regulation

Recent studies on ion regulation mechanisms of fishes have studied in zebrafish (*Danio rerio*). However, relative researches are not necessarily applicable to euryhaline fishes because of stenohaline character. Therefore, we use a suitable model, an euryhaline species, Indian medaka (*Oryzias melastigma*), could tolerate a wide range of different salinities and have biological characteristics such as small size, short life cycle, high fecundity, distinctive life stages, transparent embryos, and amenability to genetic and chemical screening would allow as a proper model animal. Compared to zebrafish, a stenohaline FW fish, medaka is a euryhaline fish and even can reproduce in SW. These advantages also made Indian medaka as a superior model organism for osmoregulation research in the teleost. (Inokuchi et al., 2017).

Previous studies have suggested that there are three types of ionocytes (NHE3 cells, NCC cells, and ECaC cells) in FW and two types of ionocytes (SW-type ionocytes and AC cells) in SW-acclimated medaka were identified. NHE cells are crucial to uptake Na^+ and secrete H^+/NH_4^+. Also, NCC cells are responsible for Na^+ and Cl^- uptake. Besides, ECaC cells play a key role for Ca^{2+} uptake. However, SW-type ionocytes were essential for acid secretion, NaCl secretion and NH_4^+ excretion, which are accompanied by smaller AC cells that express less basolateral NKA. Moreover, they would form multicellular complexes drives Na^+ across the leaky junction between the SW-type ionocytes and the AC cells by the transepithelial electrical potential. (Hsu et al., 2014; Hwang et al., 2011; Lin et al., 2012). As a result, euryhaline Indian medaka was proposed as an alternative model for research into ionic regulation during acclimation to a wide range of salinities.

1.5 Purpose

The purpose of this study is to elucidate whether IGFBPs participate in body fluid

doi:10.6342/NTU202002011

ionic homeostasis in euryhaline teleosts. We use Indian medaka (*Oryzias melastigma*) as a model examine if and how IGFBPs involved the ion regulation mechanisms, and following questions were investigated: (1) Are specific isoforms of IGFBP family involved in ion regulation and which ion is regulated? (2) Are IGFBPs specifically expressed in ionocytes? (3) Which type of ionocytes was IGFBPs expressed in medaka? (4) How do IGFBPs participate in ion regulatory mechanisms?

doi:10.6342/NTU202002011

2. Materials and methods

2.1 Experimental animals

Mature Indian medaka (*Oryzias melastigma*) were maintained in circulating tap water (FW) at 27 °C under a photoperiod of 14 h of light and 10 h of dark at the Institute of Cellular and Organismic Biology, Academia Sinica, Taipei, Taiwan. Fertilized eggs were collected and kept at 27 °C in the incubator. During the experiments, the media were replaced daily to retain water quality.

2.2 Acclimation experiments

2.2.1 SW transfer experiments

30 ‰ seawater (SW) was prepared by adding the appropriate amounts of sea salt. In SW transfer experiments, adult medaka were acclimated to the local tap water for 2 weeks, and then were exposed to 50%-diluted SW for 2 days. Finally, adult medaka were acclimated to SW to collect gills for qRT-PCR. Gills of adult medaka were collected at 0.5, 1, 2, 4 h and 7 days after transfer of the fish from the FW to SW. For embryos, fertilized eggs were directly transferred from FW to SW until 6 days post fertilization (dpf) and were sampled.

2.2.2 Low [Ca^{2+}] artificial water transfer experiments

Normal [Ca^{2+}] (0.2 mM) and low [Ca^{2+}] (0.001 mM) artificial freshwater, referred to as artificial FW and FWLCa solution, were prepared with double-deionized water containing 0.2 mM $MgSO_4$, 0.2 mM K_2HPO_4, 0.2 mM KH_2PO_4, 0.4 mM NaCl and 0.2 mM/0.001 mM $CaSO_4 \cdot 2H_2O$; normal [Ca^{2+}] (9 mM) and low [Ca^{2+}] (0.001 mM) artificial SW transfer experiment, solution was referred to as artificial SW and SWLCa respectively.

doi:10.6342/NTU202002011

They were prepared with double-deionized water containing 350 mM NaCl, 25 mM Na_2SO_4, 8 mM $NaHCO_3$, 8 mM KCl, 45 mM $MgCl_2 \cdot 6H_2O$ and 9 mM/0.001 mM $CaCl_2$.

In low [Ca^{2+}] transfer experiment, medaka embryos were raised in local tap water for 3 days, and then transferred to different artificial waters of normal/low [Ca^{2+}] until 6 dpf. The artificial waters were replaced every day to keep the ion concentrations. In low [Ca^{2+}] artificial water transfer experiments, medaka embryos were sampled at sixth days.

2.3 Bioinformatic analyses

Paralogous of *igfbp* genes in Indian medaka, and other species were collected from the Ensembl genome databases, including: human, mouse, anole lizard, chicken, xenopus, tetrodon, zebrafish, Indian medaka, Japanese medaka, tilapia, ballan wrasse, bicolor damselfish and amazon molly. The Ensembl accession numbers are as listed in Table 1. To verify the membership of identified candidates in the IGFBP family, we used Clustal omega to align the amino acid sequences available in the database, and then seeded guide tree. Guide tree was performed using an online tool, Interactive Tree Of Life (https://itol.embl.de). All of *igfbp* isoforms in the Indian medaka were cloned and sequenced before further analyses.

2.4 Preparation of total RNA

To begin with, adult medaka were anaesthetized with 0.03% ethyl 3-aminobenzoate methanesulfonate (MS-222). Then, appropriate amounts of medaka tissues were collected and immersed in 1 mL Trizol reagent (Invitrogen, Carlsbad, CA, USA) for homogenization. After chloroform extraction, total RNA was purified following the manufacturer's protocol and the quantity and quality of total RNA was determined at absorbances of 260 and 280 nm by NanoDrop ND-1000 (Thermo Scientific, San

doi:10.6342/NTU202002011

Francisco, CA). RNA was stored at -20°C until was used.

2.5 Reverse-transcription polymerase chain reaction analysis

For complementary DNA (cDNA) synthesis, 1-2.5 μg of total RNA was reverse-transcribed in a final volume of 20 μL containing 0.5 mM dNTPs, 2.5 μM oligo (dT)20, 250 ng random primers, 5 mM dithiothreitol, 40 units RNase inhibitor, and 200 units Superscript RT (Invitrogen) for 1 h at 55°C, followed by a 10 min incubation at 80°C. For PCR amplification, 1 μL cDNA was used as a template in a 25 μL final reaction volume containing 0.25 μM dNTP, 1.25 units Gen-Taq polymerase (Genemark, Taipei, Taiwan), and 0.2 μM of each primer (Table 2). Gene expression of medaka *igfbp1a, -1b, -2a, -2b, -3a, -3b, -4, -5a, -5b, -6a* and *-6b* in various organs were examined by reverse-transcription polymerase chain reaction (RT-PCR). Medaka *rpl7* was used as an internal control in RT-PCR analysis. Total RNA samples were extracted from the brain, eyes, gills, heart, intestines, kidneys, liver, muscles and spleen, of medaka.

2.6 Quantitative real-time PCR

Real-time PCR (qPCR) was performed with a Light Cycler real-time PCR system (Roche, Penzberg, Germany). The final reaction volume in each well was 10 μL, which contained 5 μL of 2X SYBR Green master mix (Integrated DNA Technologies Applied System), 20-30 ng of cDNA, and 300 nM of primer pairs. A standard curve for each gene was identified in the linear range, and the *rpl7* gene was used as an internal control. Primer was used for qPCR are provided in Table 2. To determine the specificity of the primer sets, all primer sets was confirmed by the presence of a single peak in the dissociation curve analysis, the detection of a single band of the correct size by gel electrophoresis and sequenced.

doi:10.6342/NTU202002011

2.7 Whole-mount *in situ* hybridization

Primers (Table 3) were designed against the conserved regions and used to obtain DNA fragments by PCR. These fragments were inserted into the pGEM-T Easy vector (Promega) and amplified with the T7 and SP6 primers by PCR. And then, products were used as templates for in vitro transcription with T7 or SP6 RNA polymerase respectively in the presence of digoxigenin (DIG) or fluorescein (FLU) (Roche, Penzberg, Germany). Two primers are designed to enlarge the hybridization target and enhance signal intensity. RNA probes were examined using RNA gels and NanoDrop ND-1000 (Thermo Scientific, San Francisco, CA) to confirm the quality and concentration. Medaka embryos and adult gills were fixed with 4 % paraformaldehyde in phosphate-buffered saline solution (PBS) at 4 °C overnight and then treated with methanol at 4°C overnight. Then, samples were washed with diethylpyrocarbonate (DEPC)-PBST several times and were subsequently incubated with specific probe in hybridization buffer (60% formamide, 5x SSC, 0.1% Tween 20, 500 g/mL yeast tRNA, and 50 g/mL heparin) overnight at 55°C. In the next day, samples were washed with 2× saline-sodium citrate (SSC) buffer at 55 °C for 30 min, 0.2× SSC at 55 °C for 30 min and then blocked with blocking reagent (Roche, Penzberg, Germany) at room temperature for 4h. Also, samples were incubated with an anti-DIG antibody (1:4,000) or anti-FLU antibody (1:500) at 4°C overnight in the second day. In the third day, samples were washed with PBST at room temperature for 30 min six times. Then, stained with the mixture of nitro blue tetrazolium and 5-bromo-4-chloro-3-indolyl phosphate or fluorescein-tyramide signal amplification (TSA) buffer with TSA (50:1)-(Perkin-Elmer, Boston, MA, USA) for fluorescence staining. To bleach the pigmentation, samples were treated with 0.005% (w/v) Potassium hydroxide and 3% (w/w) hydrogen peroxide in PBST after ISH. Besides, for double-labeled ISH and immunohistochemistry,

doi:10.6342/NTU202002011

the hybridized samples were further subjected to immunohistochemistry as described below.

2.8 Immunohistochemistry

After *in situ* hybridization (ISH), samples were rinsed in PBST and then blocked with 3% bovine serum albumin (BSA) for 1 h at room temperature. Afterward, samples were incubated overnight at 4°C with the primary antibodies with an α5 monoclonal antibody against the avian Na^+-K^+ ATPase (NKA) (diluted 1: 200 with PBS; Molecular Probes). After washing with PBS for 30 min, samples were incubated with an Alexa Fluor 568 goat anti-mouse antibodies (diluted 1: 200 with PBS) for 2 h at room temperature and then washed with PBST. Images were obtained with an upright microscope (Axioplan 2 Imaging; Carl Zeiss) or a Leica TCS-SP5 confocal laser scanning microscope (Leica Lasertechnik, Heidelberg, Germany).

2.9 Measurements of whole body Ca^{2+} and Na^+ contents

For Ca^{2+} and Na^+ measurements, appropriate medaka embryos (6 pdf) were rinsed with deionized water six times to eliminate skin surface ions and then were pooled as one sample. Afterward, samples were dried at 60°C for 5 h and were digested with 50 μL 70% HNO_3 at 60°C overnight. Then, digested solutions were diluted with 14% HNO_3 and the total Ca^{2+} and Na^+ contents were measured with an atomic absorption spectrophotometer (Hitachi Z-8000, Tokyo, Japan). Standard curves were made using standard solutions purchased from Merck (Merck, Darmstadt, Germany).

2.10 Scanning ion-selective electrode technique (SIET) and measurement of Ca^2

doi:10.6342/NTU202002011

gradients

Details of the SIET system were described in previous study (Hung et al., 2019). To construct Ca^{2+}-selective microelectrodes, glass capillary tubes (no. TW 150-4; World Precision Instruments, Sarasota, FL, USA) were pulled on a Sutter P-97 Flaming Brown pipette puller (Sutter Instruments, San Rafael, CA, USA) into micropipettes with tip diameters of 3–4 μm. The micropipette was then baked at 120 °C overnight and coated with dimethyl chlorosilane (Sigma-Aldrich) for 30 min. The micropipettes were backfilled with a 1-cm column of electrolytes and frontloaded with a 20–30-μm column of liquid ion exchanger cocktail (Sigma-Aldrich) to create a Ca^{2+}-selective microelectrode to measure ion fluxes on the specific and individual ionocytes of medaka larva. Putative ECaC ionocytes was distinguished with pattern and size.

The Nernstian property of each microelectrode was measured by placing the microelectrode in a series of standard solutions to calibrate the Ca^{2+}-selective probe. The SIET was performed at room temperature (26–28 °C) in a small plastic recording chamber filled with 1 ml of the recording medium. Before being measured, an anesthetized embryo was positioned in the center of the chamber with its lateral side contacting the base of the chamber. A Ca^{2+}-selective probe was moved to the target position (2 μm above the apical surface of the cells) to record ionic flux at specific ionocytes. Five to ten replicate recordings were usually performed on a neuromast, and the median value was used to calculate ionic fluxes with ASET software (Applicable Electronics). Voltage differences obtained from ASET software were converted to a concentration gradient using the following equation: $\Delta C = C_b \times 10^{(\Delta V/S)} - C_b$, where ΔC is the concentration gradient between two points, C_b is the background ion concentration, ΔV is the voltage gradient obtained from ASET software, and S is the Nernst slope of the electrode. The concentration gradient was subsequently converted to ionic flux using Fick's law of

doi:10.6342/NTU202002011

diffusion: $J = D(\Delta C)/\Delta X$, where J (pmol·cm^{-2}·s^{-1}) is the net flux of the ion, *D* is the diffusion coefficient of the ion (in FW: 13.3×10^{-6} cm^2/s for Na^+ and 20.3×10^{-6} cm^2/s for Cl^-), ΔC (pmol/cm^{-3}) is the concentration gradient, and ΔX (cm) is the distance between the two points.

2.11 Pharmacological experiment

Pharmacological experiments were performed by using the BMS-75480719 (Adooq Bioscience, Irvine, USA), a small-molecule inhibitor of IGF1R. BMS-75480719 was dissolved in dimethyl sulfoxide (DMSO) and added to artificial FWLCa solution at a final concentration of 4.8 μM. 3 dpf medaka embryos were transferred to artificial FWLCa solution until 6 dpf, and treated with 4.8μM BMS-75480719 for 1 day before sampling. Afterward, the whole-body ion contents and the ion influxes of ionocytes were analyzed.

2.12 Statistical analysis

Values are presented as means ± SD and were compared using Student's t-test. Statistical analyses were performed using GraphPad Prism 8 (GraphPad Software, San Diego, CA).

doi:10.6342/NTU202002011

3. Results

3.1 Identification paralogous of *igfbp* gene family in database

Paralogous of *igfbp* genes from different species were collected from Ensembl database (Table 1). Guide tree shows that IGFBPs have been designated six groups in mammals. However, many teleost species possess two copies of each of the five types of IGFBP family except *igfbp4.* There are total 11 *igfbp* paralogous in Indian medaka and all of them were cloned and sequenced before further analyses (Fig. 1).

3.2 Effects of salinity change on the branchial mRNA expression level of IGFBPs after transfer from FW to SW in medaka

In order to elucidate whether the IGFBPs involved in ion regulation in medaka, the expression of *igfbp*s in adult gills were analyzed by qPCR after transfer from FW to SW (Fig. 2A). The heat map shows the expression of *igfbp1a* was up-regulated, while *igfbp2a, -2b, -3a, -4, -5a, -5b, 6a,* and *-6b* were down-regulated after the seawater exposure (Fig. 2B). Among them, the expression of *igfbp5a* was down-regulated dramatically after seawater exposure. Implies that IGFBP family may be involved in the salt regulation mechanisms.

3.3 Tissue distribution of IGFBPs in adult medaka in FW

The mRNA expressions of medaka IGFBPs in various tissues were examined by RT-PCR while *rpl7* was used as an internal control. The results showed that the expression of *igfbp1b*, *-2b*, *-3b*, *-4*, *-5b*, and *-6b* were widely expressed in various tissues. While most of *igfbps* were detected being expressed in the brain. And *igfbp1b* and *igfbp2b* were highly expressed in the liver. Also, the results have found that *igfb1a*, *-1b*, *-2a*, *-2b*, *-3b*, *-4*, *-5a*,

doi:10.6342/NTU202002011

-5b, *-6a* and *-6b* were detected in the gills, but only *igfbp5a* was dominantly expressed (Fig. 3). It implies that IGF signaling may have a functional role in the gill via one of its binding protein member *igfbp5a*, probably in the ion regulation.

3.4 *igfbp5a* expressing cells localize next to NKA expressing ionocytes in FW-acclimated medaka

In order to identify whether *igfbp5a* is expressed in ionocytes, whole mount ISH was used to identify the mRNA expression patterns of *igfbp5a* (Fig. 4A and D) and immunohistochemistry of NKA, an ionocyte marker, was labeled the localization of ionocytes (Fig. 4B and E) in FW-acclimated embryos. The results revealed the *igfbp5a* expressing cells is smaller than NKA-labeled ionocytes and *igfbp5a* positive cells also exhibited weak NKA signals (Fig. 4C and F). Besides, most of *igfbp5a* expressing cells localized in the adjacent cells of NKA-labeled ionocytes. These results suggested that *igfbp5a* might expressed in a certain type of ionocytes or have a function related to the ionocytes.

3.5 Co-localization of *igfbp5a* and *trpv6* in FW-acclimated medaka

Recently, *igfbp5a*, has been identified expressing in ionocytes and play a role to maintain calcium homeostasis in zebrafish (Dai et al., 2010). Also, ECaC cells play a key role for Ca^{2+} uptake (Hwang and Lin, 2013). Therefore, to identify which type of cells was *igfbp5a* expressed in medaka, double-labeled ISH was used to analyze the mRNA expression of *igfbp5a* and *trpv6* (*ecac*) in FW-acclimated gills. The expression of *igfbp5a* is colocalized with t*rpv6* in the gills (Fig. 5A-F). These results clearly showed that *igfbp5a* is expressing in the ECaC cells, a type of ionocyte who is responsible for calcium uptake.

doi:10.6342/NTU202002011

3.6 Effects of environmental Ca^{2+} concentration on the expression of *trpv6* and *igfbp5a* in medaka embryos

To quickly elucidate whether the *igfbp5a* involves calcium homeostasis in medaka. 3 dpf medaka embryos were transferred to artificial FW, FWLCa, SW and SWLCa respectively, and then acclimated until 6 dpf (Fig. 6A). qPCR analysis showed the expression of *trpv6* was significantly increased after acclimated to FWLCa or SWLCa, however, the expression of *igfbp5a* were not affected under low [Ca^{2+}] conditions (Fig. 6B and C).

3.7 Effects of environmental Ca^{2+} concentration on *trpv6* and *igfbp5a* expressing cells in medaka embryos

To further confirm the function of *igfbp5a* in low [Ca^{2+}] water, *trpv6* and *igfbp5a* expressing cell numbers were analyzed after ISH (Fig. 7A-H). Compared with the normal [Ca^{2+}] group, acclimation to FWLCa or SWLCa solution, resulted in a robust increase of *trpv6* and *igfbp5a* expressing cells in the trunk (Fig. 7I and J). However, the effect is different in the skin of yolk sac, the number of *igfbp5a* expressing cells were increased only in FWLCa (Fig. 7L)., but *trpv6* expressing cell were increased only in SWLCa (Fig. 7K). These results suggested that the total number of *trpv6* and *igfbp5a* expressing cells were increased by low [Ca^{2+}] treatment, but the increment pattern was different between *trpv6* and *igfbp5a* expressing cells under low [Ca^{2+}] in artificial FW or SW.

3.8 Effects of blockage of the IGF signaling on the *trpv6* cell number and function

To determine whether this Ca^{2+} deficiency-induced *trpv6* cell growth was activated by IGF signaling pathway. 3 dpf embryos were transferred and acclimated to artificial FW and FWLCa solution for 3 days until 6 dpf, and 4.8 μM of BMS-754807 (a

doi:10.6342/NTU202002011

structurally distinct IGF1R inhibitors) were added 1 day before sampling to verify the effects on *trpv6* cell numbers and the Ca^{2+} influx from the ionocyte in medaka embryos. ISH data shows blockage of the IGF1R-mediated signaling significantly reduces the *trpv6* cells in both trunk and yolk area under low [Ca^{2+}] condition (Fig. 8). Besides, BMS-754807 also significantly decreased the Ca^{2+} uptake from putative ECaC ionocytes (Fig. 9). Suggested that *igfbp5a* might play a role in the regulation of IGF signaling under low [Ca^{2+}] acclimation in the *trpv6* expressing ionocytes.

3.9 Effects of blockage of the IGF signaling on the whole-body ion contents

To further explore the physiological effects on reduced ECaC cells after IGF signaling being inhibited in medaka embryos. 3 dpf embryos were transferred and acclimated to artificial FWLCa solution for 3 days until 6 dpf, and 4.8 μM BMS-754807 were added 1 day before sampling to elucidate the whole-body contents of Ca^{2+} and Na^{+}. Surprisingly, IGF signaling inhibition did not affect the whole-body contents of Ca^{2+} (Fig. 10A). However, it significantly increased the Na^{+} contents in 6 dpf embryos interestingly (Fig. 10B).

3.10 The effects of environmental Ca^{2+} concentration on various type of ionocytes

Previous study found there are three types of ionocytes (NHE3, NCC, and ECaC expressing cells) in FW-acclimated medaka (Hwang et al., 2011). We then further identified which type of ionocytes was the *igfbp5a* expressing cells neighboring in FW-acclimated medaka. And if the increased *igfbp5a* expressing cells affects the expression pattern of *nhe3* and *ncc* expressing ionocytes after low [Ca^{2+}] acclimation. Double-labeled ISH of *trpv6* and *ncc/nhe3* were co-stained with NKA IHC signals in medaka embryos. 3 dpf embryos were acclimated to artificial FW and FWLCa solution for 3 days

doi:10.6342/NTU202002011

until 6 dpf. The *trpv6* expressing cells were represent as *igfbp5a* expressing cells in a specific group of NKA-labeled ionocytes next to *nhe3* or *ncc* expressing ionocytes (Fig. 11 and 12). Interestingly, all three genes were expressed in the trunk region, but have different expression patterns in the yolk. The *nhe3* is widely distributed from anterior to posterior and numerously in the yolk, *ncc* signals were only found in few cells in the posterior most of yolk sac areas, and *trpv6* expression region were overlapping with *ncc* and partial *nhe3* signals but not until the anterior of the yolk. However, the number of *ncc*/*nhe3* expressing cells seems have no affected in low [Ca^{2+}] condition, but the results still need further investigation and analyses in the future.

doi:10.6342/NTU202002011

4. Discussion

Many studies have investigated the physiological role of IGFBP genes about regulator of growth in the teleost lineage. Knowing that the GH/IGF axis can participate in the ion regulation to promote salinity tolerance because it directly affects the mRNA expression of transporters or size and density of ionocytes (Mancera and McCormick, 1998). Besides, IGFBPs can play a key position to regulate IGF signaling globally and locally (Firth and Baxter, 2002; Taguchi and White, 2008). Therefore, we hypothesized that IGFBPs contribute to ionic regulation in an euryhaline medaka. The major findings of the present study were: (1) the first time that the observations of the salinity effects on the expressions of IGFBPs in Indian medaka; (2) identify the localization of *igfbp5a* in the ECaC cell in medaka gills and functionally related to environmental Ca^{2+} uptake; (3) blockage of the IGF signaling not only affect the number of ECaC cells, but also reduce the Ca^{2+} uptake from the putative ECaC ionocytes.

4.1 Potential of IGFBPs for ion regulation

In the present study, we successfully identified the IGFBP family and isoforms that are expressed in various tissues in Indian medaka. Based on guide tree analysis in present study (Fig. 1), IGFBPs have been designated to six groups in mammals. However, Indian medaka possess two copies of each of the five types of IGFBP family except *igfbp4.* The medaka IGFBP family has 11 genes, including *igfb1a*, *-1b*, *-2a*, *-2b*, *-3a -3b*, *-4*, *-5a*, *-5b*, *-6a* and *-6b*. The phenomenon is a common observation in many teleost and probably due to the vertebrate ancestor was experienced additional rounds of whole genome duplication. (Van et al., 2017; Macqueen and Johnston, 2014). Recent study show that the salmonid fish family has even experienced fourth whole genome duplication event in its evolutionary history and retain at least 19 unique IGFBP genes (Macqueen and Johnston,

doi:10.6342/NTU202002011

2014).

The tissue distribution of the IGFBP family in mammals has been extensively studied (Shimasaki and Ling, 1991). In mammals, *Igfbp1* and *-2* are mainly produced in the liver and secreted to circulation system, where it acts to limit IGF signaling. They are widely considered as negative regulator of somatic growth (Wood et al., 2005). In Indian medaka, we found *igfbp1b* and *igfbp2b* were also highly expressed in the liver (Fig. 3). Similar to *igfbp1a*, *-1b*, and *2b* in salmonids, are major circulatory IGFBPs and mainly expressed in the liver (Macqueen et al., 2013; Maures and Duan, 2002; Rahman and Thomas, 2017). In addition, medaka *igfbp4*, *−5,* and *−6* were highly expressed in the gill, however, only *igfbp5a* was dominantly expressed than in other tissues. In zebrafish, *igfbp5*a was expressed at high levels in gill, and lower levels in several other tissues, while *igfbp5b* was ubiquitously expressed (Garcia and Macqueen, 2018). These findings also consistent with previous study in salmon as well (Macqueen et al., 2013). Since gills has been known is a pivotal tissue for body fluid ionic homeostasis in fishes (Evans et al., 2005; Hwang et al., 2011). Currently, how branchial *igfbp* modulates ionoregulatory challenges in Indian medaka is not yet clear. We also reported the observation of the salinity effects on the expressions of branchial IGFBPs (Fig. 2). The mRNA expression of branchial *igfbp5a* and *-5b* and *-6b* were decreased after seawater exposure. It is in agreement with previous study, *igfbp5a*, *−5b1*, *−5b2,* and *−6b2* were diminished following SW exposure in Atlantic salmon (Breves et al., 2017). Besides, we also found the expression of *igfbp1a* was up-regulated, while *igfbp2a, -3a* and *-4* and were down-regulated after the seawater exposure. Based on these results, it is concluded that IGFBP family may be involved in the salt regulation mechanisms in Indian medaka and implies that IGF signaling may have a functional role in the ion regulation in medaka gills, probably via *igfbp5a*.

doi:10.6342/NTU202002011

4.2 Expression of *igfbp5a* in the ECaC ionocytes

Previous study has demonstrated that there are three types of ionocytes (NHE3 cells, NCC cells, and ECaC cells) in FW-acclimated medaka (Hwang et al., 2011). Here, we found that the *igfbp5a* expressing cells is smaller than NKA-labeled ionocytes and *igfbp5a* positive cells also exhibited weak NKA signals (Fig. 4). Importantly, most of *igfbp5a* expressing cells expressed in the adjacent cells of NKA-labeled ionocytes.

The expression pattern of *igfbp5a* in Indian medaka is similar with ECaC expressing cells in Japanese medaka (*Oryzias latipes*). Double-labeled ISH and immunocytochemistry experiments of Japanese medaka ebmryos enabled the detection of *trpv6* mRNA in a specific group of NKA-labeled ionocytes and localized in the cells adjacent to NHE expressing ionocytes (Hsu et al., 2014). In zebrafish, ECaC expressing ionocytes is responsible for Ca^{2+} uptake. Besides, recent studies have demonstrated that *igfbp5a* expressing cells were localized in the ECaC expressing cells in zebrafish (Dai et al., 2010). Therefore, to identify whether *igfbp5a* was also expressed in the ECaC cells in medaka, double-labeled ISH was performed to analyze the mRNA expression of *igfbp5a* and *trpv6* in the FW-acclimated gills. The result showed that the expression of *igfbp5a* is colocalized with t*rpv6* not only in the medaka gills (Fig. 5) but also in the embryos (data not shown). Based on these results, it is possible to assume that the function of *igfbp5a* is related to ECaC expressing ionocytes, which is associated with the uptake functions of Ca^{2+}.

4.3 Actions of IGFBP5a on Ca^{2+} homeostasis

IGFBP5 is the most highly conserved among distinct types of IGFBPs across species and has the broadest range of biological activities, it is expressed in diverse cell types in

doi:10.6342/NTU202002011

different developmental stages and various species (Schneider et al., 2002). IGFBP5 can exert the inhibition of IGF signaling by competing with the IGF1 receptor for ligand binding or potentiate of IGF signaling by delivery of IGFs to the IGF1 receptor (Allard and Duan, 2018). Different from mammals, teleost has more paralogs of *igfbp5*. In zebrafish, *igfbp5a* was expressed at high levels in and gill, and lower levels in several other tissues, while *igfbp5b* was ubiquitously expressed, suggesting evolutionary divergence in the regulatory function (Zhou et al., 2008, Dai et al., 2010). Besides, *igfbp5a* expressing cells were localized to NaR cells responsible for Ca^{2+} uptake via ECaC in zebrafish and regulate IGF signaling for the proliferation of NaR cells induced by low environmental [Ca^{2+}] for Ca^{2+} homeostasis (Dai et al., 2010). Also, ECaC kept these cells in differentiated state and functioning as Ca^{2+} transporting by controlling the quiescence-proliferation decision via IGF signaling pathway (Xin et al., 2019). In the present study, medaka *igfbp5a* is also identified being expressed in ECaC expressing cells. And the expression of *trpv6* was significantly up-regulated after acclimated to low [Ca^{2+}] environment (FWLCa or SWLCa), however, the expression of *igfbp5a* were not affected (Fig. 6). Although the number of both *igfbp5a* and *trpv6* expressing cells were stimulated following low [Ca^{2+}] treatment (Fig. 7). Consistency with the study in zebrafish, low [Ca^{2+}] treatment did not affect the expression level of *igfbp5a* in isolated zebrafish NaR cells, but the *igfbp5a* expressing cell number were significantly increased in the embryos (Dai et al., 2014, Liu et al., 2020). Based on these data, medaka *igfbp5a* also likely participated in calcium homeostasis because of co-localization with *trpv6* expressing cells together with the increasable number of *igfbp5a* expressing cells under low [Ca^{2+}] stress.

4.4 The mechanism of IGFBP5a on Ca^{2+} homeostasis

IGF ligands can bind to IGF1R to regulate many biological activities, including:

doi:10.6342/NTU202002011

proliferation, differentiation, apoptosis, growth, motility, and metastasis, etc. (Hakuno and Takahashi, 2018). In the present study, we elucidated whether IGF signaling was activated in Ca^{2+} deficiency-induced ECaC cell growth by pharmacological treatment. BMS-754807 is a pyrrolo-triazine and reversible ATP-competitive antagonist of IGF1R that can inhibit the catalytic domain of the IGF1R and blocks the activity of IGF1R (Carboni et al., 2009; Wittman et al., 2009). The results showed that the *trpv6* expressing cell number in FWLCa were significantly reduced in both trunk and yolk area after IGF signaling was blocked by BMS-754807 (Fig. 8). Furthermore, to examine whether blockage of the IGF signaling affect the physiological function of the ionocytes. The SIET experiment was performed to detect Ca^{2+} flux in the putative ECaC ionocytes. Interestingly, we found that BMS-754807 also significantly decreased the Ca^{2+} uptake from putative ECaC ionocytes under low [Ca^{2+}] condition (Fig. 9). However, Ca^{2+} content was not affected by BMS-754807 in embryos (Fig. 10A). These findings imply that IGF signaling regulate not only affect the number, but also affect the function of Ca^{2+} uptake ECaC ionocytes. And the medaka local expressed *igfbp5a* protein might facilitate the IGF ligand binding with receptors according to the study in zebrafish (Dai et al., 2010). These findings suggested that *igfbp5a* might play a role in regulate the IGF signaling pathway under low [Ca^{2+}] acclimation in ECaC cells. In addition, gastrointestinal tract, kidney also contribute to calcium (re)absorption other than the gills in teleost (Allen et al., 2011; Khanal and Nemere, 2008). Loss of function in the putative ECaC ionocytes might cause the functional compensation from other tissues for Ca^{2+} uptake without being observed a content difference significantly.

There are many hormones also participate in regulating calcium homeostasis, including: Vitamin D, parathyroid hormone, calcitonin and stanniocalcin-1 in teleost (Lin and Hwang, 2016). Stanniocalcin-1 (STC-1) was first identified in fish (Yeung et al., 2012)

doi:10.6342/NTU202002011

and is a hypocalcemic hormone to suppress Ca^{2+} uptake function by downregulating ECaC mRNA expression (Tseng et al., 2009). Recent study has elucidated that Papp-aa, a zebrafish homolog of the IGFBP protease PAPP-A, can cleavage IGFBP5a and then release IGF to activate IGF1R (Liu et al., 2020). Hence, activating IGF1 signaling and promoting the proliferation of NaR ionocytes in response to low [Ca^{2+}] stress. On the other hand, overexpression of human STC-1 in a subset of NaR cells inhibit low [Ca^{2+}] stress-induced NaR cell proliferation in zebrafish embryos, indicating the importance of the local endogenous Papp-aa in NaR cells (Liu et al., 2020). However, if Papp-aa also involved in the [Ca^{2+}]-dependent regulation of the ECaC cell number in Indian medaka is unclear.

4.5 Potential of IGFBP5a for Na^+ regulation

Surprisingly, we found that Na^+ contents significantly increased when the IGF signaling was blocked by BMS-754807 in 6 dpf embryos acclimated to low [Ca^{2+}] in artificial FW (Fig. 10B). This result likely caused by other ionocytes responsible for Na^+ uptake. In Japanese medaka, both NHE expressing ionocytes and NCC expressing ionocytes were labeled by NKA and were associated with acclimation in the freshwater (Hsu et al., 2014). Besides, as discussed above, *trpv6* expressing cells were represent as *igfbp5a* expressing cells next to NKA-labeled ionocytes (Fig. 4). We found most of *trpv6* expressing cells were localized next to *nhe3* expressing ionocytes in Indian medaka (Fig. 11). The same with the results in Japanese medaka, *trpv6* expressing cells also localized next to *nhe3* expressing cells (Hsu et al., 2014). Interestingly, we also found partial of *trpv6* expressing ionocytes were accompanied with NCC expressing cells (Fig. 12). Besides, three genes have different expression patterns in the yolk. The *nhe3* is widely distributed and numerously in the yolk, *ncc* signals were only detected in few cells at the

doi:10.6342/NTU202002011

posterior most of yolk sac areas, and *trpv6* expression region were overlapping with *ncc* and partial *nhe3* signals but not until the anterior of the yolk. However, the number of *ncc*/*nhe3* expressing cells seems have no affected in low [Ca^{2+}] condition. However, the effects of expression pattern and cell quantification analyses in low [Ca^{2+}] were needed in the future.

IGF1 has been studied to influence on ionoregulatory functions in fishes transferred from FW to SW (McCormick et al., 2013). Besides, in *vitro* experiments have demonstrated that renal Na^+ reabsorption and epithelial sodium channel (ENaC) activity are increased by IGF1 signaling (Holzman, et al., 2007; Ilatovskaya, et al., 2015). ENaC plays a major role in sodium transport in amphibians and amniotes (lizards, crocodiles, birds, and mammals) (Hanukoglu and Hanukoglu, 2016). Although, teleost has lost ENaC genes, they may have a conserved mechanism about Na^+ hemostasis regulated by IGF signaling. Besides, another type of IGFBP protease, Papp-a2, that also can cleave IGFBP5 in mammalian cells. (Overgaard et al., 2001). High level of IGFBP5 was expressed in renal cortex, and Papp-a2 was specifically colocalized with NKCC2 and NCC in the rat renal cortex. NKCC2 and NCC are responsible for reabsorbing sodium. (Cowley et al., 2016). As a result, although the sodium homeostasis regulated by IGF signaling in mammals, the specific role of IGFBP5 and IGFBP protease in sodium homeostasis of teleost is not yet clear, that could serve as a hypothesis for the mechanism of sodium homeostatic in teleost.

4.6 ECaC cells presumed AC cells

Euryhaline fishes are able to tolerate within a wide range of salinities contributed to their ionocytes which have specific types and distinct ion-transporting proteins for different functions in FW and SW respectively. (Hirose et al., 2003; Evans et al., 2005;

doi:10.6342/NTU202002011

Hwang and Lee, 2007). SW medaka have one predominant type of SW ionocyte accompanied by smaller AC cells that exhibited weaker NKA signals and fail to stain strongly for NKCC or CFTR (Shen et al., 2011; Marshall et al., 2017). Such studies suggest that the ECaC cells may be AC cells, which were initially identified in SW teleosts (Hootman and Philpott, 1980). AC cells and the accompanying ionocytes share the same apical crypt in SW teleosts and form leaky junctions to secrete Na^+. (Hootman and Philpott, 1980; Hwang and Hirano, 1985). However, the clear role of accessory cells is poorly understood (Evans et al., 2005). In our present finding discussed above, *trpv6* expressing cells were representing in a specific group of NKA-labeled ionocytes next to *nhe3 or ncc* expressing ionocytes (Fig. 11 and 12). Also, expression of *ecac* mRNA was significantly lower in SW-acclimated embryo as compared to FW-acclimated embryo confirmed by both qPCR and ISH (Fig. 6A and 7). Similar effect has been studied in previous study in Japanese medaka (Hsu et al., 2014). Based on these results, indicate that *trpv6* mRNA is expressed in the presumed AC cells (i.e., ECaC-expressing ionocytes) of FW medaka and is regulated during FW/SW adaptation. ECaC has recently been reported to be important for Ca^{2+} absorption in the ionocytes of zebrafish and trout (Shahsavarani et al., 2006; Liao et al., 2007). Besides, a kinase involved in ion transport regulation, with-no-lysine kinase (WNK1), that was present in ion transporting cells in fish acclimated to FW and SW. WNK1 could be an indicator to specifically stain accessory cells (Marshall et al., 2017). The function of AC cells in Ca^{2+} handling during FW/SW adaptation or the specific indicator for AC cells need to investigate in the future, and this may provide a new line for AC cell function.

doi:10.6342/NTU202002011

5. Conclusion and perspectives

In summary, the present study provides that medaka Igfbp5a may play a role in Ca^{2+} homeostasis. *igfbp5a* was specifically expressed in the ECaC cell in medaka gills/skin and can be stimulated when embryo medaka were transferred to low [Ca^{2+}] environment. This action may regulate by IGF signaling, and thus participating in ionocytes responsible for Ca^{2+} uptake. IGFBP5 was conserved in many species, implying that the function of IGFBP5a on Ca^{2+} regulatory maybe conserved among vertebrates during environmental acclimation. The present findings further explore the role of IGFBP5a in the physiological acclimation to low [Ca^{2+}] stress. In the future, several issues need to be elucidated: (1) whether IGFBP5a directly participate in Ca^{2+} uptake via IGF signaling, (2) whether IGFBP5a regulates the expression or function of ion transporters related to salt absorption (e.g. NHE3 and NCC) and (3) whether *igfbp5a* expressing cells is the AC cells in SW acclimated medaka. These further studies would give new insights into fish ion regulation.

doi:10.6342/NTU202002011

References

Allard, J. B., & Duan, C. (2018). IGF-Binding Proteins: Why Do They Exist and Why Are There So Many? *Front Endocrinol* **117**.

Allen, P. J., Weihrauch, D., Grandmaison, V., Dasiewicz, P., Peake, S. J., & Anderson, W. G. (2011). The influence of environmental calcium concentrations on calcium flux, compensatory drinking and epithelial calcium channel expression in a freshwater cartilaginous fish. *J Exp Biol* **214**, 996-1006.

Baxter, R. C. (2014). IGF binding proteins in cancer: mechanistic and clinical insights. *Nat Rev Cancer* **14**, 329-341.

Breves, J. P., Fujimoto, C. K., Phipps-Costin, S. K., Einarsdottir, I. E., Bjornsson, B. T., & McCormick, S. D. (2017). Variation in branchial expression among insulin-like growth-factor binding proteins (*igfbps*) during Atlantic salmon smoltification and seawater exposure. *BMC Physiol* **17**.

Cao, Y. B., Chen, X. Q., Wang, S., Chen, X. C., Wang, Y. X., Chang, J. P., & Du, J. Z. (2009). Growth hormone and insulin-like growth factor of naked carp (*Gymnocypris przewalskii*) in Lake Qinghai: expression in different water environments. *Gen Comp Endocrinol* **161**, 400-406.

Carboni, J. M., Wittman, M., Yang, Z., Lee, F., Greer, A., Hurlburt, W., & Gottardis, M. M. (2009). BMS-754807, a small molecule inhibitor of insulin-like growth factor-1R/IR. *Mol Cancer Ther* **8**, 3341-3349.

Clemmons, D. R. (2001). Use of mutagenesis to probe IGF-binding protein structure/function relationships. *Endocr Rev* **22**, 800-817.

Clemmons, D. R. (2016). Role of IGF Binding Proteins in Regulating Metabolism. *Trends Endocrinol Metab* **27**, 375-391.

doi:10.6342/NTU202002011

Cowley, A. W., Jr., Yang, C., Kumar, V., Lazar, J., Jacob, H., Geurts, A. M., & Liang, M. (2016). Pappa2 is linked to salt-sensitive hypertension in Dahl S rats. *Physiol Genomic* **48**, 62-72.

Dai, W., Bai, Y., Hebda, L., Zhong, X., Liu, J., Kao, J., & Duan, C. (2014). Calcium deficiency-induced and TRP channel-regulated IGF1R-PI3K-Akt signaling regulates abnormal epithelial cell proliferation. *Cell Death Differ* **21**, 568-581.

Dai, W., Kamei, H., Zhao, Y., Ding, J., Du, Z., & Duan, C. (2010). Duplicated zebrafish insulin-like growth factor binding protein-5 genes with split functional domains: evidence for evolutionarily conserved IGF binding, nuclear localization, and transactivation activity. *FASEB J* **24**, 2020-2029.

Daza, D. O., Sundstrom, G., Bergqvist, C. A., Duan, C., & Larhammar, D. (2011). Evolution of the insulin-like growth factor binding protein (IGFBP) family. *Endocrinology* **152**, 2278-2289.

Deane, E. E., Kelly, S. P., Lo, C. K., & Woo, N. Y. (1999). Effects of GH, prolactin and cortisol on hepatic heat shock protein 70 expression in a marine teleost *Sparus sarba*. *J Endocrinol* **161**, 413-421.

Denley, A., Cosgrove, L. J., Booker, G. W., Wallace, J. C., & Forbes, B. E. (2005). Molecular interactions of the IGF system. *Cytokine Growth Factor Rev* **16**, 421-439.

Duan, C., & Plisetskaya, E. M. (1993). Nutritional regulation of insulin-like growth factor-I mRNA expression in salmon tissues. *J Endocrinol* **139**, 243-252.

Duan, C., Ren, H., & Gao, S. (2010). Insulin-like growth factors (IGFs), IGF receptors, and IGF-binding proteins: roles in skeletal muscle growth and differentiation. *Gen Comp Endocrinol* **167**, 344-351.

Duan, C., & Xu, Q. (2005). Roles of insulin-like growth factor (IGF) binding proteins in regulating IGF actions. *Gen Comp Endocrinol* **142**, 44-52.

doi:10.6342/NTU202002011

Evans, D. H., Piermarini, P. M., & Choe, K. P. (2005). The multifunctional fish gill: dominant site of gas exchange, osmoregulation, acid-base regulation, and excretion of nitrogenous waste. *Physiol Rev* **85**, 97-177.

Firth, S. M., & Baxter, R. C. (2002). Cellular actions of the insulin-like growth factor binding proteins. *Endocr Rev* **23**, 824-854.

Garcia de la Serrana, D., & Macqueen, D. J. (2018). Insulin-Like Growth Factor-Binding Proteins of Teleost Fishes. *Front Endocrinol* **9**, 80.

Hakuno, F., & Takahashi, S. I. (2018). IGF1 receptor signaling pathways. *J Mol Endocrinol* **61**, 69-86.

Hanukoglu, I., & Hanukoglu, A. (2016). Epithelial sodium channel (ENaC) family: Phylogeny, structure-function, tissue distribution, and associated inherited diseases. *Gene* **579**, 95-132.

Hiroi, J., Kaneko, T., & Tanaka, M. (1999). *In vivo* sequential changes in chloride cell morphology in the yolk-sac membrane of mozambique tilapia (*Oreochromis mossambicus*) embryos and larvae during seawater adaptation. *J Exp Biol* **202**, 3485-3495.

Hiroi, J., McCormick, S. D., Ohtani-Kaneko, R., & Kaneko, T. (2005). Functional classification of mitochondrion-rich cells in euryhaline Mozambique tilapia (*Oreochromis mossambicus*) embryos, by means of triple immunofluorescence staining for Na^+/K^+-ATPase, $Na^+/K^+/2Cl^-$ cotransporter and CFTR anion channel. *J Exp Biol* **208**, 2023-2036.

Hiroi, J., Yasumasu, S., McCormick, S. D., Hwang, P. P., & Kaneko, T. (2008). Evidence for an apical Na-Cl cotransporter involved in ion uptake in a teleost fish. *J Exp Biol* **211**, 2584-2599.

Hirose, S., Kaneko, T., Naito, N., & Takei, Y. (2003). Molecular biology of major

doi:10.6342/NTU202002011

components of chloride cells. *Comp Biochem Physiol B Biochem Mol Biol* **136**, 593-620.

Hoeflich, A., Wu, M., Mohan, S., Foll, J., Wanke, R., Froehlich, T., & Wolf, E. (1999). Overexpression of insulin-like growth factor-binding protein-2 in transgenic mice reduces postnatal body weight gain. *Endocrinology* **140**, 5488-5496.

Hoenderop, J. G., Nilius, B., & Bindels, R. J. (2005). Calcium absorption across epithelia. *Physiol Rev* **85**, 373-422.

Holick, M. F. (2007). Vitamin D deficiency. *N Engl J Med* **357**, 266-281.

Holzman, J. L., Liu, L., Duke, B. J., Kemendy, A. E., & Eaton, D. C. (2007). Transactivation of the IGF-1R by aldosterone. *Am J Physiol Renal Physiol* **292**, 1219-1228.

Hootman, S. R., & Philpott, C. W. (1980). Accessory cells in teleost branchial epithelium. *Am J Physiol* **238**, 199-206.

Hsu, H. H., Lin, L. Y., Tseng, Y. C., Horng, J. L., & Hwang, P. P. (2014). A new model for fish ion regulation: identification of ionocytes in freshwater- and seawater-acclimated medaka (*Oryzias latipes*). *Cell Tissue Res* **357**, 225-243.

Hung, G. Y., Wu, C. L., Chou, Y. L., Chien, C. T., Horng, J. L., & Lin, L. Y. (2019). Cisplatin exposure impairs ionocytes and hair cells in the skin of zebrafish embryos. *Aquat Toxicol* **209**, 168-177.

Hwang, P. P., & Hirano, R. (1985). Effects of Environmental Salinity on Intercellular Organization and Junctional Structure of Chloride Cells in Early Stages of Teleost Development. *J Exp Zool* **236**, 115-126.

Hwang, P. P., & Lee, T. H. (2007). New insights into fish ion regulation and mitochondrion-rich cells. *Comp. Biochem Physiol A Mol Integr Physiol* **148**, 479-497.

doi:10.6342/NTU202002011

Hwang, P. P., Lee, T. H., & Lin, L. Y. (2011). Ion regulation in fish gills: recent progress in the cellular and molecular mechanisms. *Am J Physiol Regul Integr Comp Physiol* **301**, 28-47.

Hwang, P. P., & Lin, L. Y. (2013). Gill ionic transport, acid-base regulation, and nitrogen excretion. *The physiology of fishes,* **edn 4,** 205-233. Eds D. H. Evans., & J. B. Claiborne. Boca Raton: CRC Press.

Ilatovskaya, D. V., Levchenko, V., Brands, M. W., Pavlov, T. S., & Staruschenko, A. (2015). Cross-talk between insulin and IGF-1 receptors in the cortical collecting duct principal cells: implication for ENaC-mediated Na^+ reabsorption. *Am J Physiol Renal Physiol* **308**, 713-719.

Imai, Y., Busby, W. H., Jr., Smith, C. E., Clarke, J. B., Garmong, A. J., Horwitz, G. D., & Clemmons, D. R. (1997). Protease-resistant form of insulin-like growth factor-binding protein 5 is an inhibitor of insulin-like growth factor-I actions on porcine smooth muscle cells in culture. *J Clin Invest* **100**, 2596-2605.

Inokuchi, M., Hiroi, J., Watanabe, S., Lee, K. M., & Kaneko, T. (2008). Gene expression and morphological localization of NHE3, NCC and NKCC1 a in branchial mitochondria-rich cells of Mozambique tilapia (*Oreochromis mossambicus*) acclimated to a wide range of salinities. *Comp Biochem Physiol A Mol Integr Physiol* **151**, 151-158.

Inokuchi, M., Nakamura, M., Miyanishi, H., Hiroi, J., & Kaneko, T. (2017). Functional classification of gill ionocytes and spatiotemporal changes in their distribution after transfer from seawater to freshwater in Japanese seabass. *J Exp Biol* **220**, 4720-4732.

Jepsen, M. R., Kloverpris, S., Mikkelsen, J. H., Pedersen, J. H., Fuchtbauer, E. M., Laursen, L. S., & Oxvig, C. (2015). Stanniocalcin-2 inhibits mammalian growth by proteolytic inhibition of the insulin-like growth factor axis. *J Biol Chem* **290**, 3430-

doi:10.6342/NTU202002011

3439.

Jones, J. I., & Clemmons, D. R. (1995). Insulin-like growth factors and their binding proteins: biological actions. *Endocr Rev* **16**, 3-34.

Khanal, R. C., & Nemere, I. (2008). Regulation of intestinal calcium transport. *Annu Rev Nutr* **28,** 179-196.

Kloverpris, S., Mikkelsen, J. H., Pedersen, J. H., Jepsen, M. R., Laursen, L. S., Petersen, S. V., & Oxvig, C. (2015). Stanniocalcin-1 Potently Inhibits the Proteolytic Activity of the Metalloproteinase Pregnancy-associated Plasma Protein-A. *J Biol Chem* **29**, 21915-21924.

Kusakabe, M., Ishikawa, A., Ravinet, M., Yoshida, K., Makino, T., Toyoda, A., & Kitano, J. (2017). Genetic basis for variation in salinity tolerance between stickleback ecotypes. *Mol Ecol* **26**, 304-319.

Laursen, L. S., Overgaard, M. T., Soe, R., Boldt, H. B., Sottrup-Jensen, L., Giudice, L. C., & Oxvig, C. (2001). Pregnancy-associated plasma protein-A (PAPP-A) cleaves insulin-like growth factor binding protein (IGFBP)-5 independent of IGF: implications for the mechanism of IGFBP-4 proteolysis by PAPP-A. *FEBS Let* **504**, 36-40.

Liao, B. K., Deng, A. N., Chen, S. C., Chou, M. Y., & Hwang, P. P. (2007). Expression and water calcium dependence of calcium transporter isoforms in zebrafish gill mitochondrion-rich cells. *BMC Genomics* **8**, 354.

Liebert, A. M., & Schreck, C. B. (2006). Effects of acute stress on osmoregulation, feed intake, IGF-1, and cortisol in yearling steelhead trout (*Oncorhynchus mykiss*) during seawater adaptation. *Gen Comp Endocrinol* **148**, 195-202.

Lin, C. C., Lin, L. Y., Hsu, H. H., Thermes, V., Prunet, P., Horng, J. L., & Hwang, P. P. (2012). Acid secretion by mitochondrion-rich cells of medaka (*Oryzias latipes*)

doi:10.6342/NTU202002011

acclimated to acidic freshwater. *Am J Physiol Regul Integr Comp Physiol* **302**, 283-291.

Lin, C. H., & Hwang, P. P. (2016). The Control of Calcium Metabolism in Zebrafish (*Danio rerio*). *Int J Mol Sci* **17**, 1783.

Liu, C., Li, S., Noer, P. R., Kjaer-Sorensen, K., Juhl, A. K., Goldstein, A., & Duan, C. (2020). The metalloproteinase Papp-aa controls epithelial cell quiescence-proliferation transition. *Elife* **9**, e52322.

Macqueen, D. J., Garcia de la Serrana, D., & Johnston, I. A. (2013). Evolution of ancient functions in the vertebrate insulin-like growth factor system uncovered by study of duplicated salmonid fish genomes. *Mol Biol Evol* **30**, 1060-1076.

Macqueen, D. J., & Johnston, I. A. (2014). A well-constrained estimate for the timing of the salmonid whole genome duplication reveals major decoupling from species diversification. *Proc Biol Sci* **281**, 2881.

Mancera, J. M., & McCormick, S. D. (1998). Evidence for growth hormone/insulin-like growth factor I axis regulation of seawater acclimation in the euryhaline teleost *Fundulus heteroclitus*. *Gen Comp Endocrinol* **111**, 103-112.

Marshall, W. S., Cozzi, R. R. F., & Spieker, M. (2017). WNK1 and p38-MAPK distribution in ionocytes and accessory cells of euryhaline teleost fish implies ionoregulatory function. *Biol Open* **6**, 956-966.

Maures, T. J., & Duan, C. (2002). Structure, developmental expression, and physiological regulation of zebrafish IGF binding protein-1. *Endocrinology* **143**, 2722-2731.

McCormick, S. D., Dickhoff, W. W., Duston, J., Nishioka, R. S., & Bern, H. A. (1991). Developmental differences in the responsiveness of gill Na^+, K^+-ATPase to cortisol in salmonids. *Gen Comp Endocrinol* **84**, 308-317.

McCormick, S. D., Regish, A. M., Christensen, A. K., & Bjornsson, B. T. (2013).

doi:10.6342/NTU202002011

Differential regulation of sodium-potassium pump isoforms during smolt development and seawater exposure of Atlantic salmon. *J Exp Biol* **216**, 1142-1151.

Overgaard, M. T., Boldt, H. B., Laursen, L. S., Sottrup-Jensen, L., Conover, C. A., & Oxvig, C. (2001). Pregnancy-associated plasma protein-A2 (PAPP-A2), a novel insulin-like growth factor-binding protein-5 proteinase. *J Biol Chem* **276**, 21849-21853.

Oxvig, C. (2015). The role of PAPP-A in the IGF system: location, location, location. *J Cell Commun Signal* **9**, 177-187.

Pelis, R. M., & McCormick, S. D. (2001). Effects of growth hormone and cortisol on Na^+-K^+-$2Cl^-$ cotransporter localization and abundance in the gills of Atlantic salmon. *Gen Comp Endocrinol* **124**, 134-143.

Pellissier, T., Al Nafea, H., & Good, S. V. (2018). Divergence of insulin superfamily ligands, receptors and Igf binding proteins in marine versus freshwater stickleback: Evidence of selection in known and novel genes. *Comp Biochem Physiol Part D Genomics Proteomics* **25**, 53-61.

Perrot, V., Moiseeva, E. B., Gozes, Y., Chan, S. J., & Funkenstein, B. (2000). Insulin-like growth factor receptors and their ligands in gonads of a hermaphroditic species, the gilthead seabream (*Sparus aurata*): expression and cellular localization. *Biol Reprod* **63**, 229-241.

Rahman, M. S., & Thomas, P. (2017). Molecular and biochemical responses of hypoxia exposure in Atlantic croaker collected from hypoxic regions in the northern Gulf of Mexico. *PLoS One* **12**, e0184341.

Reindl, K. M., & Sheridan, M. A. (2012). Peripheral regulation of the growth hormone-insulin-like growth factor system in fish and other vertebrates. *Comp. Biochem Physiol A Mol Integr Physiol* **163**, 231-245

doi:10.6342/NTU202002011

Reinecke, M. (2010). Influences of the environment on the endocrine and paracrine fish growth hormone-insulin-like growth factor-I system. *J Fish Biol* **76**, 1233-1254.

Reinecke, M., Bjornsson, B. T., Dickhoff, W. W., McCormick, S. D., Navarro, I., Power, D. M., & Gutierrez, J. (2005). Growth hormone and insulin-like growth factors in fish: where we are and where to go. *Gen Comp Endocrinol* **142**, 20-24.

Schneider, M. R., Wolf, E., Hoeflich, A., & Lahm, H. (2002). IGF-binding protein-5: flexible player in the IGF system and effector on its own. *J Endocrinol* **172**, 423-440.

Seidelin, M., & Madsen, S. S. (1999). Endocrine control of Na^+, K^+-ATPase and chloride cell development in brown trout (*Salmo trutta*): interaction of insulin-like growth factor-I with prolactin and growth hormone. *J Endocrinol* **162**, 127-135.

Seidelin, M., Madsen, S. S., Byrialsen, A., & Kristiansen, K. (1999). Effects of insulin-like growth factor-I and cortisol on Na^+, K^+-ATPase expression in osmoregulatory tissues of brown trout (*Salmo trutta*). *Gen Comp Endocrinol* **113**, 331-342.

Shahsavarani, A., McNeill, B., Galvez, F., Wood, C. M., Goss, G. G., Hwang, P. P., & Perry, S. F. (2006). Characterization of a branchial epithelial calcium channel (ECaC) in freshwater rainbow trout (*Oncorhynchus mykiss*). *J Exp Biol* **209**, 1928-1943.

Shamblott, M. J., & Chen, T. T. (1992). Identification of a second insulin-like growth factor in a fish species. *Proc Natl Acad Sci U S A* **89**, 8913-8917.

Shen, W. P., Horng, J. L., & Lin, L. Y. (2011). Functional plasticity of mitochondrion-rich cells in the skin of euryhaline medaka larvae (*Oryzias latipes*) subjected to salinity changes. *Am J Physiol Regul Integr Comp Physiol* **300**, 858-868.

Shepherd, B. S., Drennon, K., Johnson, J., Nichols, J. W., Playle, R. C., Singer, T. D., & Vijayan, M. M. (2005). Salinity acclimation affects the somatotropic axis in rainbow trout. *Am J Physiol Regul Integr Comp Physiol* **288**, 1385-1395.

doi:10.6342/NTU202002011

Shepherd, B. S., Sakamoto, T., Nishioka, R. S., Richman, N. H., 3rd, Mori, I., Madsen, S. S., & Grau, E. G. (1997). Somatotropic actions of the homologous growth hormone and prolactins in the euryhaline teleost, the tilapia, *Oreochromis mossambicus*. *Proc Natl Acad Sci U S A* **94**, 2068-2072.

Shimasaki, S., & Ling, N. (1991). Identification and molecular characterization of insulin-like growth factor binding proteins (IGFBP-1, -2, -3, -4, -5 and -6). *Prog Growth Factor Res* **3**, 243-266.

Siwanowicz, I., Popowicz, G. M., Wisniewska, M., Huber, R., Kuenkele, K. P., Lang, K., & Holak, T. A. (2005). Structural basis for the regulation of insulin-like growth factors by IGF binding proteins. *Structure* **13**, 155-167.

Skou, J. C., & Esmann, M. (1992). The Na^+, K^+-ATPase. *J Bioenerg Biomembr* **24**, 249-261.

Taguchi, A., & White, M. F. (2008). Insulin-like signaling, nutrient homeostasis, and life span. *Annu Rev Physiol* **70**, 191-212.

Tang, Y. L., Shepherd, B. S., Nichols, A. J., Dunham, R., & Chen, T. T. (2001). Influence of environmental salinity on messenger RNA levels of growth hormone, prolactin, and somatolactin in pituitary of the channel catfish (*Ictalurus punctatus*). *Mar Biotechnol* **3**, 205-217.

Taniyama, N., Kaneko, N., Inatani, Y., Miyakoshi, Y., & Shimizu, M. (2016). Effects of seawater transfer and fasting on the endocrine and biochemical growth indices in juvenile chum salmon (*Oncorhynchus keta*). *Gen Comp Endocrinol* **236**, 146-156.

Tseng, D. Y., Chou, M. Y., Tseng, Y. C., Hsiao, C. D., Huang, C. J., Kaneko, T., & Hwang, P. P. (2009). Effects of stanniocalcin 1 on calcium uptake in zebrafish (*Danio rerio*) embryo. *Am J Physiol Regul Integr Comp Physiol* **296**, R549-557.

Upton, Z., Chan, S. J., Steiner, D. F., Wallace, J. C., & Ballard, F. J. (1993). Evolution of

doi:10.6342/NTU202002011

insulin-like growth factor binding proteins. *Growth Regu* **3**, 29-32.

Van de Peer, Y., Mizrachi, E., & Marchal, K. (2017). The evolutionary significance of polyploidy. *Nat Rev Genet* **18**, 411-424.

Wittman, M. D., Carboni, J. M., Yang, Z., Lee, F. Y., Antman, M., Attar, R., &. Vyas, D. M. (2009). Discovery of a 2,4-disubstituted pyrrolo[1,2-f] [1,2,4] triazine inhibitor (BMS-754807) of insulin-like growth factor receptor (IGF-1R) kinase in clinical development. *J Med Chem* **52**, 7360-7363.

Wood, A. W., Duan, C., & Bern, H. A. (2005). Insulin-like growth factor signaling in fish. *Int Rev Cytol* **243**, 215-285.

Xin, Y., Malick, A., Hu, M., Liu, C., Batah, H., Xu, H., & Duan, C. (2019). Cell-autonomous regulation of epithelial cell quiescence by calcium channel Trpv6. *Elife* **8**, e48003.

Yeung, B. H., Law, A. Y., & Wong, C. K. (2012). Evolution and roles of stanniocalcin. *Mol Cell Endocrinol* **349**, 272-280.

Zheng, G. D., Zhou, C. X., Lin, S. T., Chen, J., Jiang, X. Y., & Zou, S. M. (2017). Two grass carp (*Ctenopharyngodon idella*) insulin-like growth factor-binding protein 5 genes exhibit different yet conserved functions in development and growth. *Comp Biochem Physiol B Biochem Mol Biol* **204**, 69-76.

Zhou, J., Li, W., Kamei, H., & Duan, C. (2008). Duplication of the *IGFBP-2* gene in teleost fish: protein structure and functionality conservation and gene expression divergence. *PLoS One* **3**, e3926.

doi:10.6342/NTU202002011

Tables and figures

Table 1. Summary of known orthologs of IGFBP1 and IGFBP6

IGFBP1 orthologs			IGFBP2 orthologs		
Species	**Protein name**	**Accession numbers**	**Species**	**Protein name**	**Accession numbers**
Human *(Homo sapiens)*	IGFBP1	ENSG00000146678	Human *(Homo sapiens)*	IGFBP2	ENSG00000115457
Mouse *(Mus musculus)*	IGFBP1	ENSMUSG00000020429	Mouse *(Mus musculus)*	IGFBP2	ENSMUSG00000039323
Chicken (*Gallus gallus*)	IGFBP1	ENSGALG00000043493	Chicken (*Gallus gallus*)	IGFBP2	ENSGALG00000011469
Anole lizard (*Anolis carolinensis*)	IGFBP1	ENSACAG00000008063	Xenopus (*Xenopus tropicalis*)	IGFBP2	ENSXETG00000019875
Xenopus (*Xenopus tropicalis*)	IGFBP1	ENSXETG00000015656	Tetraodon (*Tetraodon nigroviridis*)	IGFBP2a	ENSTNIG00000008344
Tetraodon (*Tetraodon nigroviridis*)	IGFBP1a	ENSTNIG00000000228	Tetraodon (*Tetraodon nigroviridis*)	IGFBP2b	ENSTNIG00000008865
Tetraodon (*Tetraodon nigroviridis*)	IGFBP1b	ENSTNIG00000000894	Zebrafish *(Danio rerio)*	IGFBP2a	ENSDARG00000052470
Zebrafish *(Danio rerio)*	IGFBP1a	ENSDARG00000099351	Zebrafish *(Danio rerio)*	IGFBP2b	ENSDARG00000031422
Zebrafish *(Danio rerio)*	IGFBP1b	ENSDARG00000038666	**Indian medaka (*Oryzias melastigma*)**	IGFBP2a	ENSOMEG00000014012
Indian medaka (*Oryzias melastigma*)	IGFBP1a	ENSOMEG00000014831	**Indian medaka (*Oryzias melastigma*)**	IGFBP2b	ENSOMEG00000020645
Indian medaka (*Oryzias melastigma*)	IGFBP1b	ENSOMEG00000004680	Japanese medaka HdrR (*Oryzias latipes*)	IGFBP2a	ENSORLG00000022125
Japanese medaka HdrR (*Oryzias latipes*)	IGFBP1a	ENSORLG00000024957	Japanese medaka HdrR (*Oryzias latipes*)	IGFBP2b	ENSORLG00000014695
Japanese medaka HdrR (*Oryzias latipes*)	IGFBP1b	ENSORLG00000017161	Tilapia (*Oreochromis niloticus*)	IGFBP2a	ENSONIG00000013363
Tilapia (*Oreochromis niloticus*)	IGFBP1a	ENSONIG00000006369	Tilapia (*Oreochromis niloticus*)	IGFBP2b	ENSONIG00000004666
Tilapia (*Oreochromis niloticus*)	IGFBP1b	ENSONIG00000009667	Ballan wrasse (*Labrus bergylta*)	IGFBP2a	ENSLBEG00000014348
Ballan wrasse (*Labrus bergylta*)	IGFBP1a	ENSLBEG00000025619	Ballan wrasse (*Labrus bergylta*)	IGFBP2b	ENSLBEG00000005611
Ballan wrasse (*Labrus bergylta*)	IGFBP1b	ENSLBEG00000017546	Bicolor damselfish (*Stegastes partitus*)	IGFBP2a	ENSSPAG00000007262
Bicolor damselfish (*Stegastes partitus*)	IGFBP1a	ENSSPAG00000005534	Amazon molly(*Poecilia formosa*)	IGFBP2a	ENSPFOG00000014380
Bicolor damselfish (*Stegastes partitus*)	IGFBP1b	ENSSPAG00000006670	Amazon molly(*Poecilia formosa*)	IGFBP2b	ENSPFOG00000014498
Amazon molly(*Poecilia formosa*)	IGFBP1a	ENSPFOG00000023943			
Amazon molly(*Poecilia formosa*)	IGFBP1b	ENSPFOG00000000389			

doi:10.6342/NTU202002011

IGFBP3 orthologs			IGFBP4 orthologs		
Species	**Protein name**	**Accession numbers**	**Species**	**Protein name**	**Accession numbers**
Human *(Homo sapiens)*	IGFBP3	ENSG00000146674	Human *(Homo sapiens)*	IGFBP4	ENSG00000141753
Mouse *(Mus musculus)*	IGFBP3	ENSMUSG00000020427	Mouse *(Mus musculus)*	IGFBP4	ENSMUSG00000017493
Chicken (*Gallus gallus*)	IGFBP3	ENSGALG00000037940	Chicken (*Gallus gallus*)	IGFBP4	ENSGALG00000040672
Anole lizard (*Anolis carolinensis*)	IGFBP3	ENSACAG00000008077	Anole lizard (*Anolis carolinensis*)	IGFBP4	ENSACAG00000016160
Tetraodon (*Tetraodon nigroviridis*)	IGFBP3a	ENSTNIG00000006450	Xenopus (*Xenopus tropicalis*)	IGFBP4	ENSXETG00000021361
Tetraodon (*Tetraodon nigroviridis*)	IGFBP3b	ENSTNIG00000003211	Tetraodon (*Tetraodon nigroviridis*)	IGFBP4	ENSTNIG00000014149
Zebrafish *(Danio rerio)*	IGFBP3	ENSDARG00000099144	**Indian medaka (*Oryzias melastigma*)**	IGFBP4	ENSOMEG00000019551
Indian medaka (*Oryzias melastigma*)	IGFBP3a	ENSOMEG00000014843	Japanese medaka HdrR (*Oryzias latipes*)	IGFBP4	ENSORLG00000002661
Indian medaka (*Oryzias melastigma*)	IGFBP3b	ENSOMEG00000004654	Ballan wrasse (*Labrus bergylta*)	IGFBP4	ENSLBEG00000016814
Japanese medaka HdrR (*Oryzias latipes*)	IGFBP3a	ENSORLG00000022715	Bicolor damselfish (*Stegastes partitus*)	IGFBP4	ENSSPAG00000002306
Japanese medaka HdrR (*Oryzias latipes*)	IGFBP3b	ENSORLG00000017149	Amazon molly(*Poecilia formosa*)	IGFBP4	ENSPFOG00000000425
Tilapia (*Oreochromis niloticus*)	IGFBP3a	ENSONIG00000006363			
Tilapia (*Oreochromis niloticus*)	IGFBP3b	ENSONIG00000009669			
Ballan wrasse (*Labrus bergylta*)	IGFBP3a	ENSLBEG00000025636			
Ballan wrasse (*Labrus bergylta*)	IGFBP3b	ENSLBEG00000017562			
Bicolor damselfish (*Stegastes partitus*)	IGFBP3a	ENSSPAG00000005471			
Bicolor damselfish (*Stegastes partitus*)	IGFBP3b	ENSSPAG00000006646			
Amazon molly(*Poecilia formosa*)	IGFBP3a	ENSPFOG00000014498			
Amazon molly(*Poecilia formosa*)	IGFBP3b	ENSPFOG00000022181			

doi:10.6342/NTU202002011

IGFBP5 orthologs			IGFBP6 orthologs		
Species	**Protein name**	**Accession numbers**	**Species**	**Protein name**	**Accession numbers**
Human *(Homo sapiens)*	IGFBP5	ENSG00000115461	Human *(Homo sapiens)*	IGFBP6	ENSG00000167779
Mouse *(Mus musculus)*	IGFBP5	ENSMUSG00000026185	Mouse *(Mus musculus)*	IGFBP6	ENSMUSG00000023046
Chicken (*Gallus gallus*)	IGFBP5	ENSGALG00000011468	Tetraodon (*Tetraodon nigroviridis*)	IGFBP6b	ENSTNIG00000002914
Xenopus (*Xenopus tropicalis*)	IGFBP5	ENSXETG00000019879	Zebrafish *(Danio rerio)*	IGFBP6a	ENSDARG00000070941
Tetraodon (*Tetraodon nigroviridis*)	IGFBP5a	ENSTNIG00000008343	Zebrafish *(Danio rerio)*	IGFBP6b	ENSDARG00000090833
Zebrafish *(Danio rerio)*	IGFBP5a	ENSDARG00000039264	**Indian medaka (*Oryzias melastigma*)**	IGFBP6a	ENSOMEG00000022000
Zebrafish *(Danio rerio)*	IGFBP5b	ENSDARG00000025348	**Indian medaka (*Oryzias melastigma*)**	IGFBP6b	ENSOMEG00000014169
Indian medaka (*Oryzias melastigma*)	IGFBP5a	ENSOMEG00000013983	Japanese medaka HdrR (*Oryzias latipes*)	IGFBP6b	ENSORLG00000025346
Indian medaka (*Oryzias melastigma*)	IGFBP5b	ENSOMEG00000020658	Tilapia (*Oreochromis niloticus*)	IGFBP6b	ENSONIG00000016561
Japanese medaka HdrR (*Oryzias latipes*)	IGFBP5a	ENSORLG00000002243	Ballan wrasse (*Labrus bergylta*)	IGFBP6b	ENSLBEG00000002443
Japanese medaka HdrR (*Oryzias latipes*)	IGFBP5b	ENSORLG00000030103	Bicolor damselfish (*Stegastes partitus*)	IGFBP6b	ENSSPAG00000004927
Tilapia (*Oreochromis niloticus*)	IGFBP5a	ENSONIG00000013364	Amazon molly(*Poecilia formosa*)	IGFBP6b	ENSPFOG00000019589
Tilapia (*Oreochromis niloticus*)	IGFBP5b	ENSONIG00000004668			
Ballan wrasse (*Labrus bergylta*)	IGFBP5a	ENSLBEG00000014331			
Ballan wrasse (*Labrus bergylta*)	IGFBP5b	ENSLBEG00000005579			
Bicolor damselfish (*Stegastes partitus*)	IGFBP5a	ENSSPAG00000007269			
Bicolor damselfish (*Stegastes partitus*)	IGFBP5b	ENSSPAG00000020902			
Amazon molly(*Poecilia formosa*)	IGFBP5a	ENSPFOG00000014348			
Amazon molly(*Poecilia formosa*)	IGFBP5b	ENSPFOG00000014472			

doi:10.6342/NTU202002011

Table 2. Primers used for RT-PCR and qPCR

Gene symbol	RT-PCR Primer sequence (5'-3')	qPCR Primer sequence (5'-3')
igfbp1a	F: CTGTAGATGCCGAGTGCCCTTA R: CCCACATGGACAGTGTACCTGA	F: CTGTAGATGCCGAGTGCCCTTA R: CCCACATGGACAGTGTACCTGA
igfbp1b	F: ATGACGGACAAGAAGAAGCCGT R: GAATGGCGTTGACCTTGGCTTT	
igfbp2a	F: ACACAGCGCAGATCTAGCATGA R: CCGGGTTCTAATCCTTTCCGGT	F: ACACAGCGCAGATCTAGCATGA R: CCGGGTTCTAATCCTTTCCGGT
igfbp2b	F: CGGCGGAGAACATGATTGGATG R: GTAGACCCCACAGAACTCACCC	F: CGGCGGAGAACATGATTGGATG R: GTAGACCCCACAGAACTCACCC
igfbp3a	F: CCTGGAGAGCCAATGAGAGGAC R: TTTTCCCCATACACCCATCCCC	F: CCTGGAGAGCCAATGAGAGGAC R: TTTTCCCCATACACCCATCCCC
igfbp3b	F: GATGTGTTCAGACAGGCACAGC R: AGTTCTGTGGGTCGGTGATGAG	
igfbp4	F: TGGTGTGTGGATCCGAAGACG R: AAGCTGGTTTTGGATTCCCCGA	F: TGGTGTGTGGATCCGAAGACG R: AAGCTGGTTTTGGATTCCCCGA
igfbp5a	F: CCAGGAAAGGACTCGCCACTAA R: GTCTTCTGCAGGGCCCAAATTC	F: CCAGGAAAGGACTCGCCACTAA R: GTCTTCTGCAGGGCCCAAATTC
igfbp5b	F: CCAGGCATAGACTACACCGGAG R: GTCATGTGGTGGGTGAAGGGTA	F: CCAGGCATAGACTACACCGGAG R: GTCATGTGGTGGGTGAAGGGTA
igfbp6a	F: AGTGTTGGTGTGTGGACGAGAA R: CTGACTGAAGGAGGAGCAGCTT	F: AGTGTTGGTGTGTGGACGAGAA R: CTGACTGAAGGAGGAGCAGCTT
igfbp6b	F: GTGCCAACGAAGACGGTACTTT R: GGGCAGTTGTCTAGAACATGCG	F: GTGCCAACGAAGACGGTACTTT R: GGGCAGTTGTCTAGAACATGCG
trpv6		F: CAGGTTGCTGCTGTTTCTTTAC R: TCGGAATCTGACTTTGTGTAGTT
rpl7	F: CATCAGGATCCGAGGTATCAAC R: CACAGACTTCAAGTTGGGGTAT	F: CATCAGGATCCGAGGTATCAAC R: CACAGACTTCAAGTTGGGGTAT

doi:10.6342/NTU202002011

Table 3. Primers used for cloning for ISH

Gene symbol	Primer sequence (5'-3')
igfbp5a	F: AAATGTCTGGCAGTGGGCAT R: GCAGAATGGCGTTGTTGAGG F2: AAACGGCGAGGAGAAGC R2: TTGCTGATGCTTGGGATTCTA
trpv6	F: ACCCTCTTCTCCGAGTTTGAGC R: TGCTCCATCTCCAGACCCAAAG F2: CTGTGCGTCCACCAACATCTTC R2: CAGGCTGTCCGAGTAAGTCACA
ncc	F: TACAGCACCATCGACCTGGT R: TTGGAGGAATAAATGTTCCCA
nhe3	F: CCCTCTGTGAGTCTGGAAATG R: ACTGGTGACGTCCATCTTTAG

doi:10.6342/NTU202002011

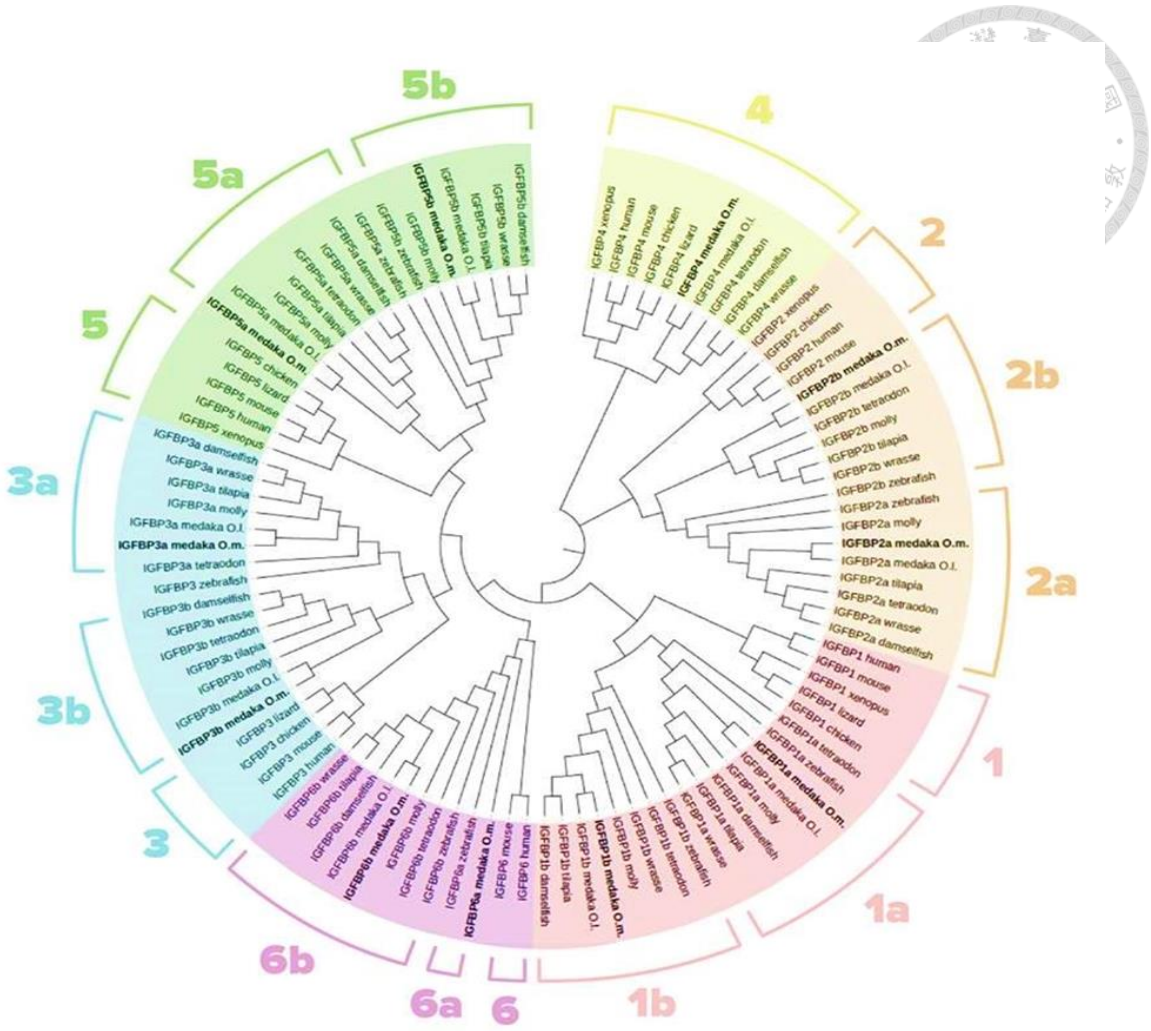

Fig. 1. Phylogenetic analysis of the *igfbp* gene family. Guide tree was generated by Clustal omega. The relationships among conventional IGFBP family and fish specific IGFBP family are shown. The IGFBPs accession numbers of Indian medaka *(Oryzias melastigma*) include: IGFBP1a, ENSOMEG00000014831; IGFBP1b, ENSOMEG00000004680; IGFBP2a, ENSOMEG00000014012; IGFBP2b, ENSOMEG00000020645; IGFBP3a, ENSOMEG00000014843; IGFBP3b, ENSOMEG00000004654; IGFBP4, ENSOMEG00000019551; IGFBP5a, ENSOMEG00000013983; IGFBP5b, ENSOMEG00000020658; IGFBP6a, ENSOMEG00000022000; IGFBP6b, ENSOMEG00000014169. The Ensembl accession numbers of other species are provided in Table 1.

doi:10.6342/NTU202002011

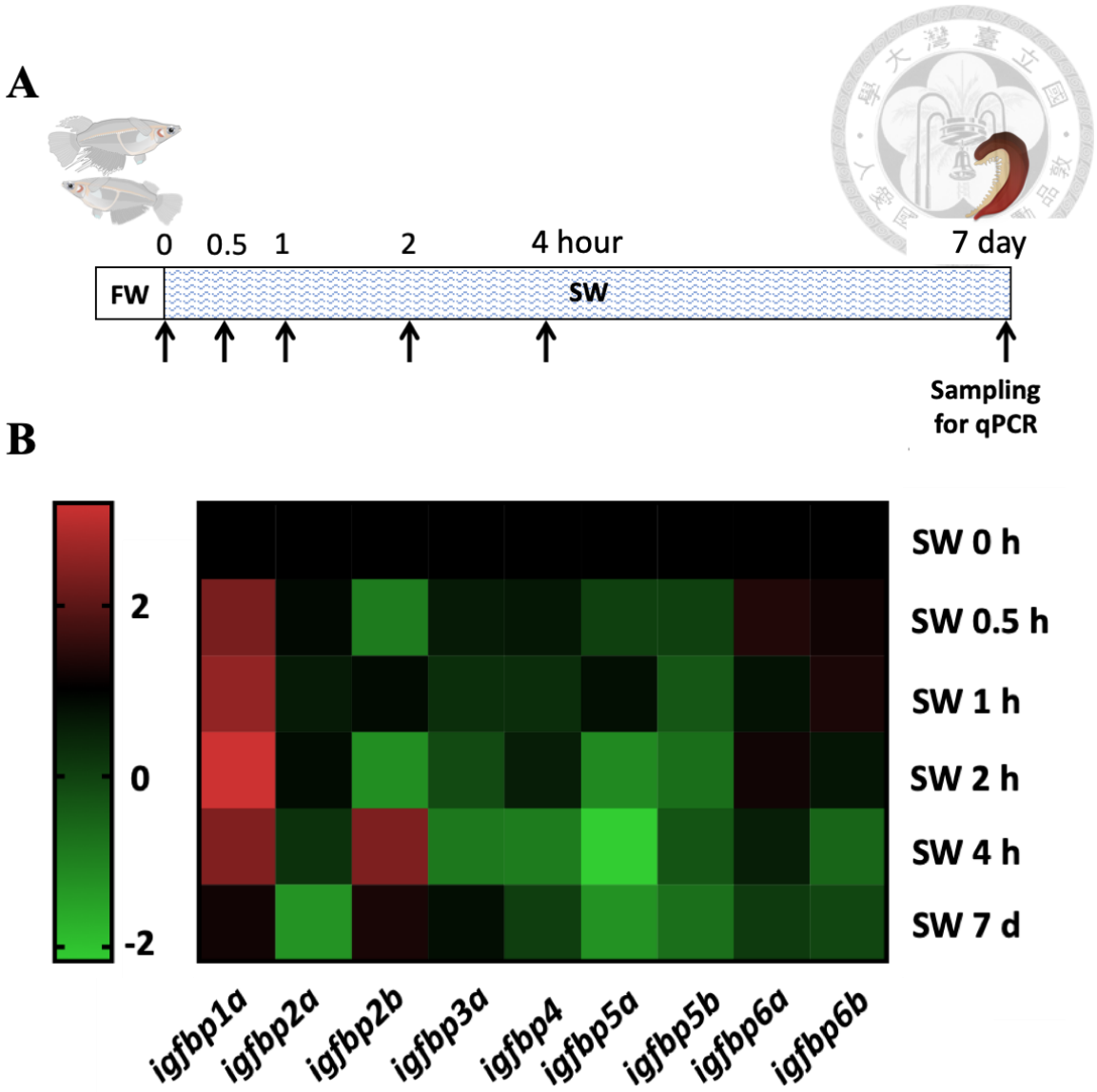

Fig. 2. Heatmap visualization of qPCR analysis of the expression of IGFBPs in medaka gills after acclimated in seawater for different times. The mRNA expression level of *igfbps* in gills were analyzed after transfer from FW to SW for different time period. The diagram of the experimental design is shown in (A). And expression level was transformed to log2 expression fold-change after normalized to SW 0 h time point (B). Red color implied expression increased while green color implied expression decreased. The expression of *igfbp1a* was up-regulated, while *igfbp2a*, *-2b*, *-3a*, *-4*, *-5a*, *-5b*, *-6a* and *-6b* and were down-regulated after the seawater exposure. The mRNA

doi:10.6342/NTU202002011

expression levels were analyzed by quantitative PCR and normalized by the *rpl7*. Values are the mean (n=6).

doi:10.6342/NTU202002011

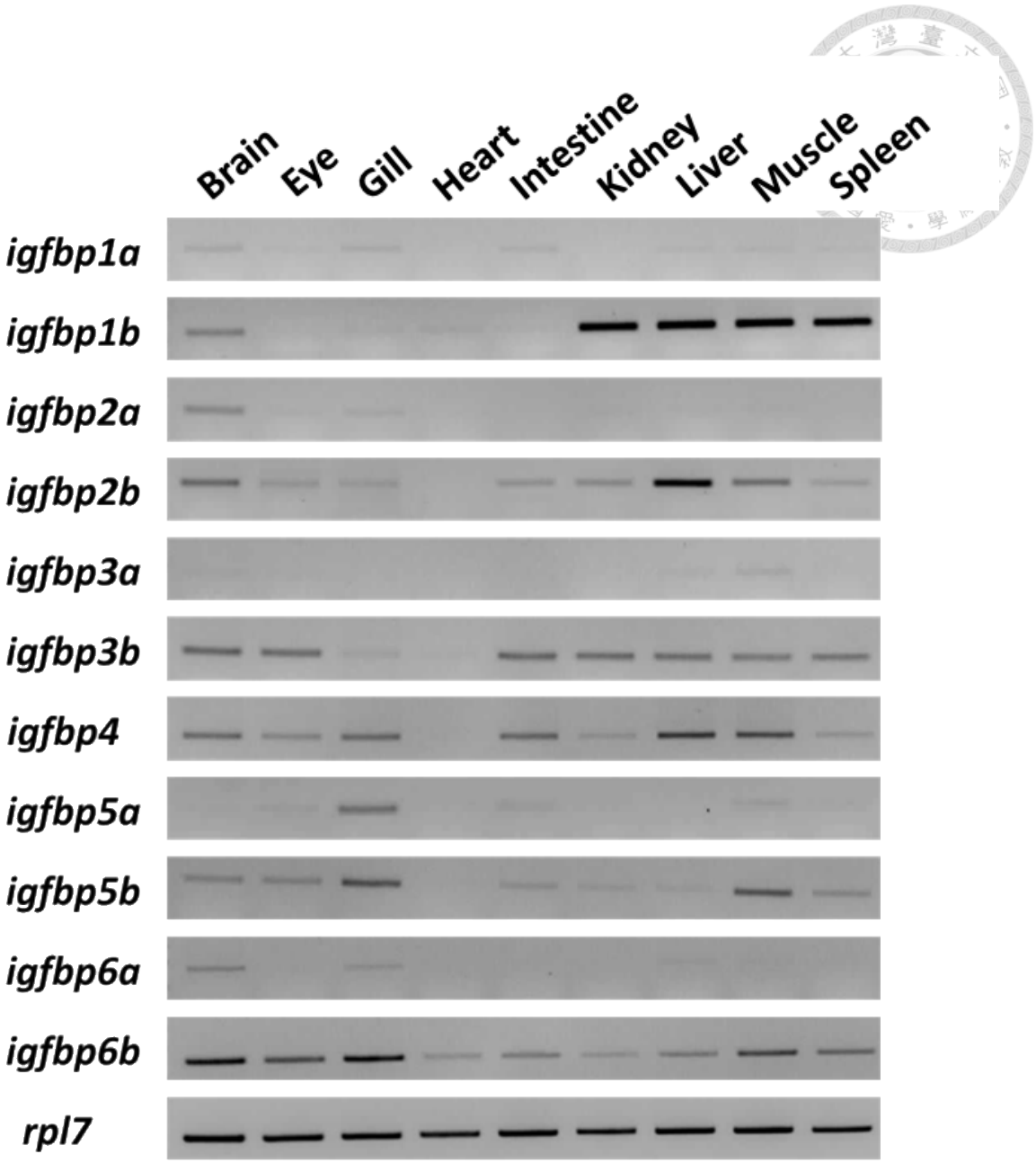

Fig. 3. Tissue distribution of IGFBPs in FW medaka. The mRNA expression levels of *igfbp* gene family were analyzed in various tissues in adult medaka by semi-quantitative PCR. These results showed *igfb1a*, *-1b*, *-2a*, *-2b*, *-3b*, *-4*, *-5a*, *-5b*, *-6a* and *-6b* were expressed in the gills, but only *igfbp5a* was dominantly expressed. *rpl7* was used as an internal control.

doi:10.6342/NTU202002011

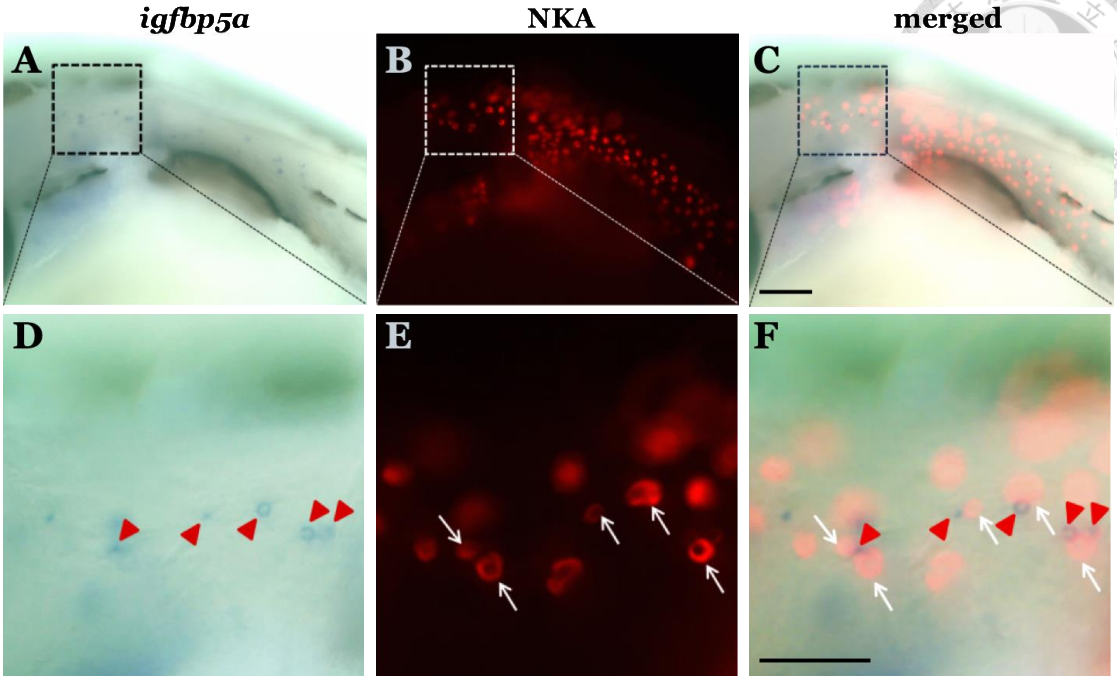

Fig. 4. Localization of *igfbp5a* and NKA in FW medaka embryos. The expression of *igfbp5a* was identified by *in situ* hybridization (A) and ionocytes were labeled by immunostaining of NKA antibody (B) in 6 dpf FW medaka embryos. Merged image were showed in (C). (D-F) are the partial enlarged images from (A-C) respectively. *igfbp5a* exhibited an ionocyte-like expression pattern (salt-and-pepper) (D) in the cells next to the NKA-labeled ionocytes. The size of *igfbp5a* expressing cells were smaller than NKA-labeled ionocytes and some *igfbp5a* positive cells also exhibited weak NKA signals. *Arrowheads* indicate cells expressing *igfbp5a* signals and *arrows* indicate cells expressing NKA protein. Scale bar indicates 50 μm in D, E, and F, and 100 μm in A, B, and C.

doi:10.6342/NTU202002011

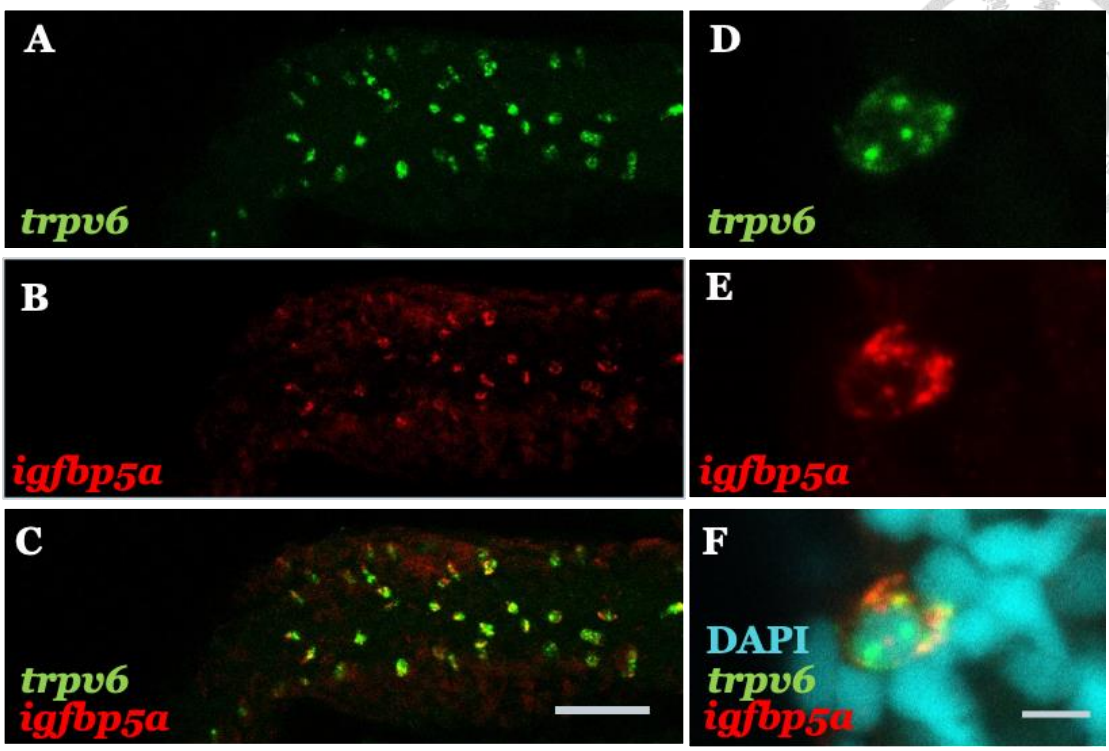

Fig. 5. Localization of *igfbp5a* and *trpv6* in medaka FW gills. The expression signals of *trpv6* (A and D) and *igfbp5a* (B and E) were analyzed by double-labeled ISH in the gills (A-F). DAPI staining labeled the cell nuclei (F). Merged images were also shown (C and F). The mRNA signals of *igfbp5a* were co-localized with the *trpv6* both in the adult gills. *Arrowheads* indicate *igfbp5a* expressing cells and *arrows* indicate *trpv6* expressing cells. Scale bar indicates 5 μm in D, E, and F, and 50 μm in A, B and C.

doi:10.6342/NTU202002011

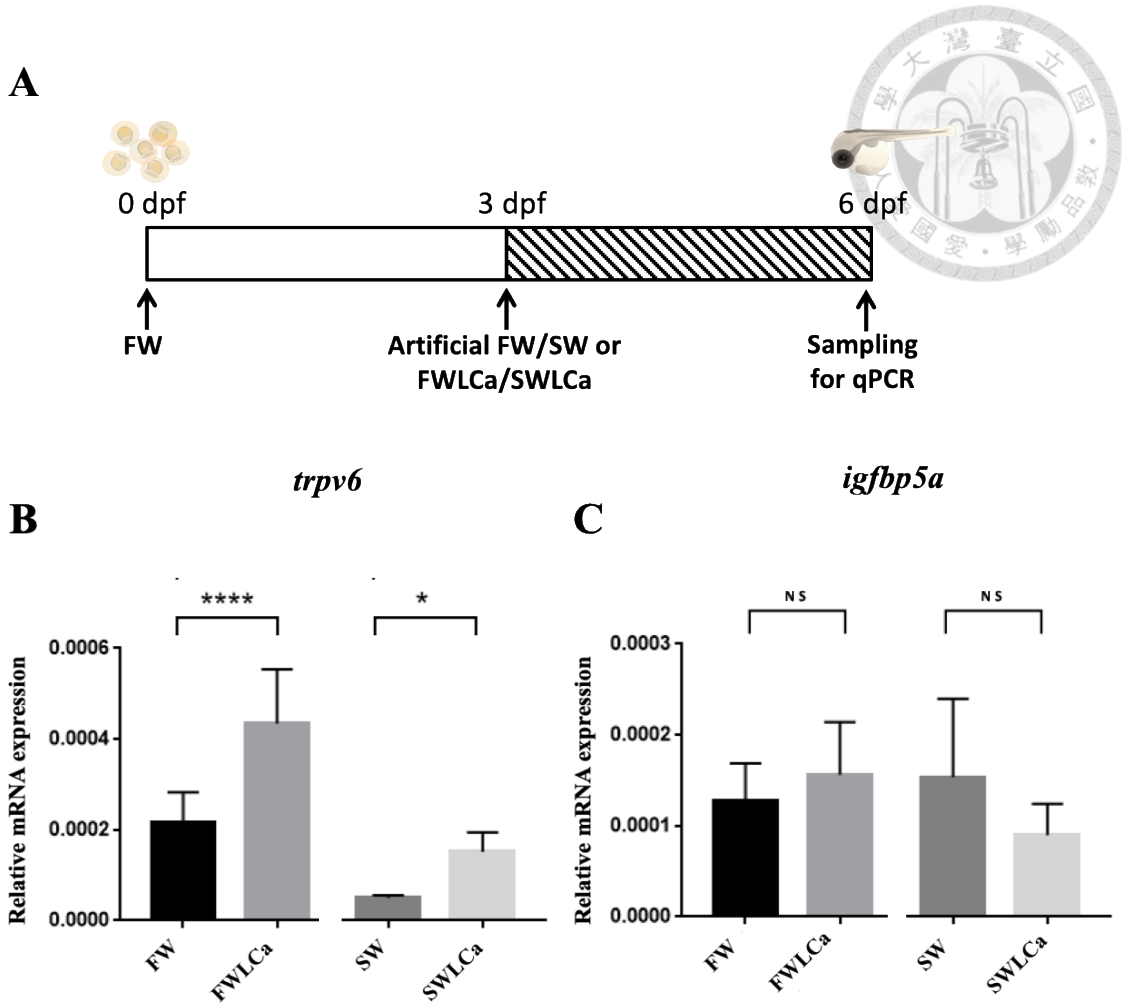

Fig. 6. Real-time PCR analysis of *trpv6* and *igfbp5a* mRNA expression in medaka embryos acclimated to low [Ca^{2+}] treatment. Diagram of the experimental design (A). 0 dpf medaka were raised in FW until 3 dpf. They were transferred to the artifical FW/SW or FWLCa/SWLCa acclimation for 3 days and sampling for qPCR afterwards. The expression of *trpv6* (B) and *igfbp5a* (C) were analyzed in 6 dpf medaka embryos by qPCR after artificial FW/SW or FWLCa/SWLCa acclimation for 3 days. The expression of *trpv6* was increased in FWLCa or SWLCa when compared with FW or SW, respectively. *igfbp5a* does not show any difference of expression after low [Ca^{2+}] acclimation. The mRNA expression levels were analyzed by quantitative PCR and normalized by the *rpl7* levels. Values are the mean ± SD (n = 10). Student's *t*-test, *$p < 0.05$, ***$p < 0.001$, ****$p < 0.0001$, and NS indicates no significant difference.

doi:10.6342/NTU202002011

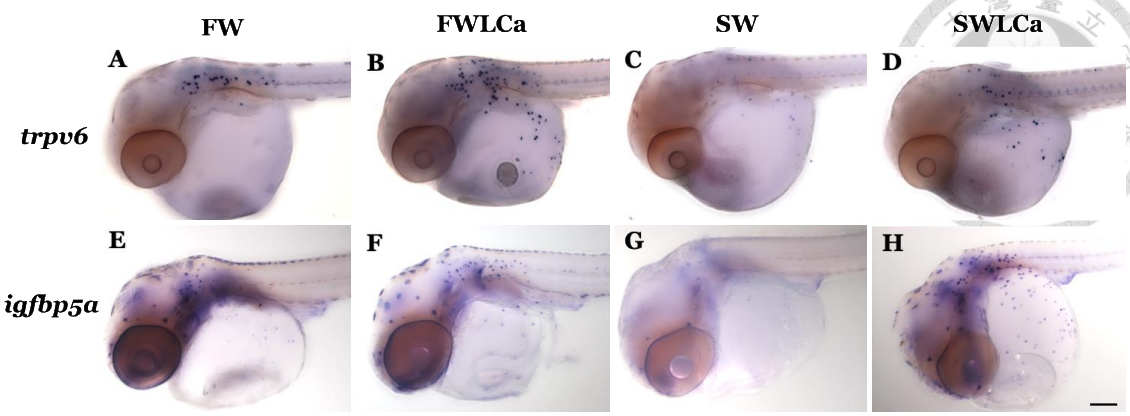

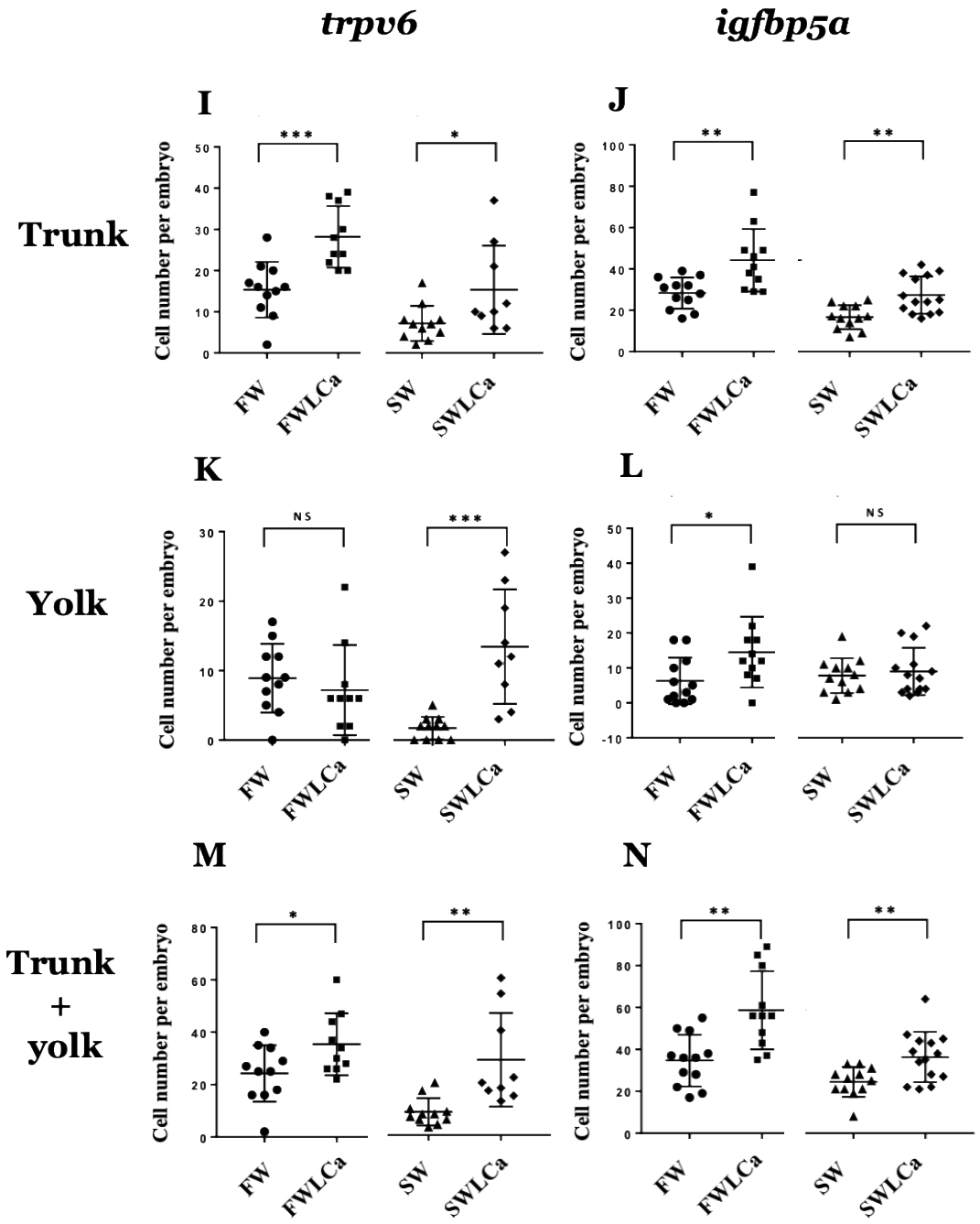

doi:10.6342/NTU202002011

Fig. 7. Effects of Low [Ca^{2+}] treatment on the number of *trpv6* and *igfbp5a* expressing cells. The expression pattern of *trpv6* (A-D) and *igfbp5a* (E-H) were analyzed in 6 dpf medaka embryos by *in situ* hybridization after normal [Ca^{2+}] artificial FW/SW or low [Ca^{2+}] artificial FWLCa/SWLCa acclimation for 3 days. Cell number of *trpv6* (I, K and M) and *igfbp5a* (J, L and N) expressing cells were then analyzed in the respective area of trunk (I and J), yolk (K and L), and trunk+yolk (M and N). Comparing with artificial FW and SW, the expressing cell numbers of *trpv6* and *igfbp5a* in artificial FWLCa and SWLCa were increased respectively in the trunk and trunk+yolk area, but *trpv6* expressing cells only increased in SWLCa and *igfbp5a* expressing cells only increased in FWLCa in the yolk area. Scale bar indicates 100 μm. Values are the mean ± SD (n >10). Student's *t*-test, *$p < 0.05$, **$p < 0.01$, ***$p < 0.001$, ****$p < 0.0001$, and NS indicates no significant difference.

doi:10.6342/NTU202002011

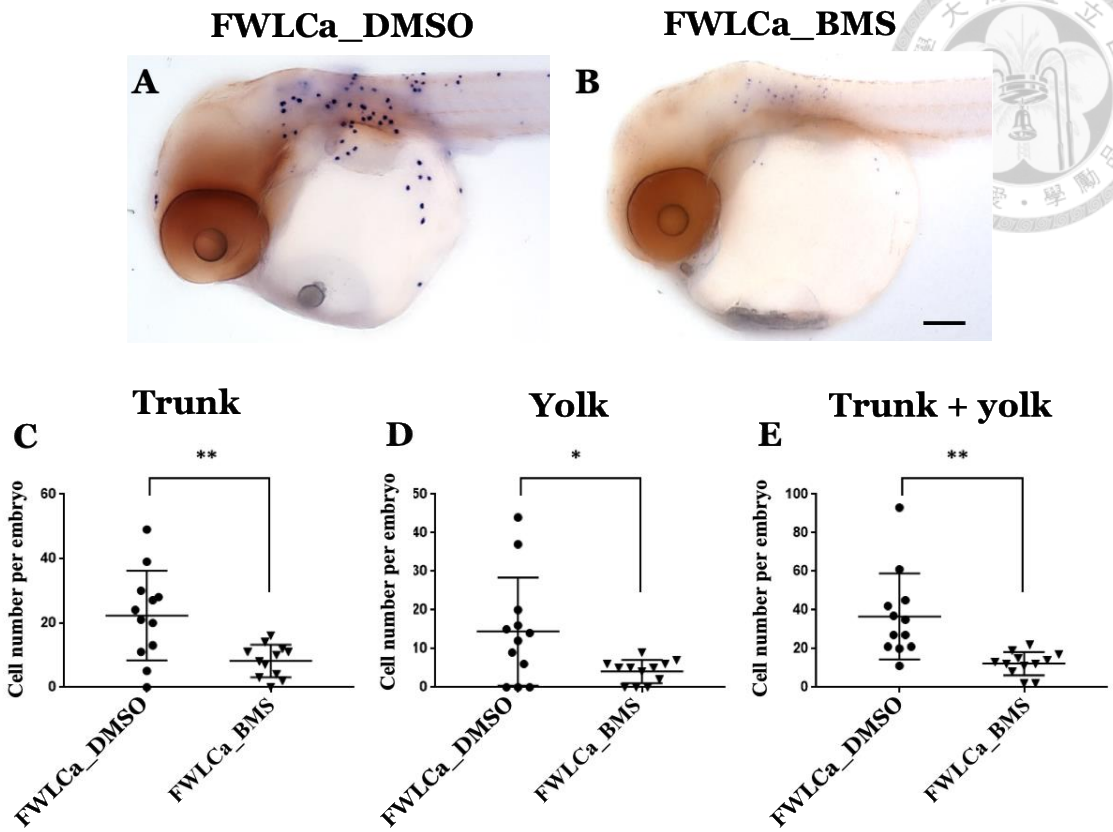

Fig.8. Effects of BMS-754807 on *trpv6* cell number in FWLCa acclimated embryos. The expression of *trpv6* were analyzed in 6 dpf medaka embryos by *in situ* hybridization after 3 days FWLCa acclimation without (A) or with BMS-754807 treatment (B) for 1 day before sampling. DMSO were added as vehicle control. The *trpv6* expressing cell number in FWLCa were significantly reduced in trunk (C), yolk (D) and trunk+yolk (E) area after IGF signaling was blocked by BMS-754807. Scale bar indicates 100 μm in A and B. Values are the mean ± SD (n =12). Student's *t*-test, *$p < 0.05$, **$p < 0.01$.

doi:10.6342/NTU202002011

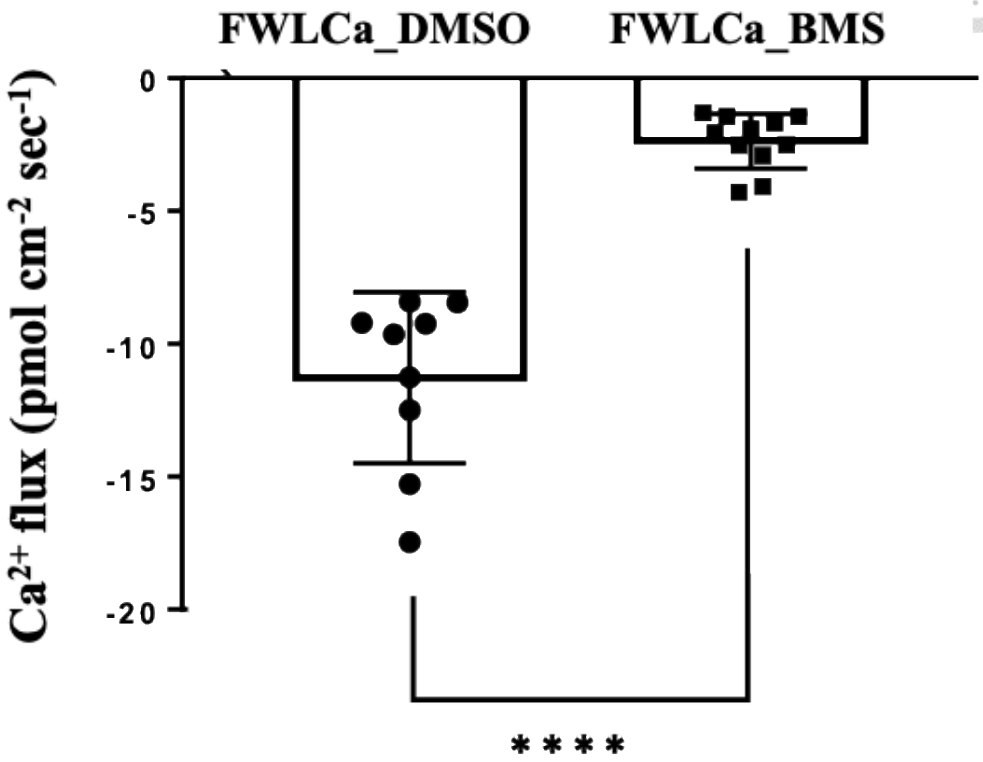

Fig. 9. Effects of BMS-754807 on cellular Ca^{2+} influxes in FWLCa acclimated embryos. The Ca^{2+} influx was measured in 6 dpf medaka embryos by SIET after 3 days FWLCa acclimation with BMS-754807 treatment for 1 day. DMSO were added as vehicle control. Ca^{2+} influxes of ionocytes were significantly decreased in BMS-754807 treatment group while compared with control. Values are the mean ± SD (n>9). Student's, *t*-test, ****$p < 0.0001$.

doi:10.6342/NTU202002011

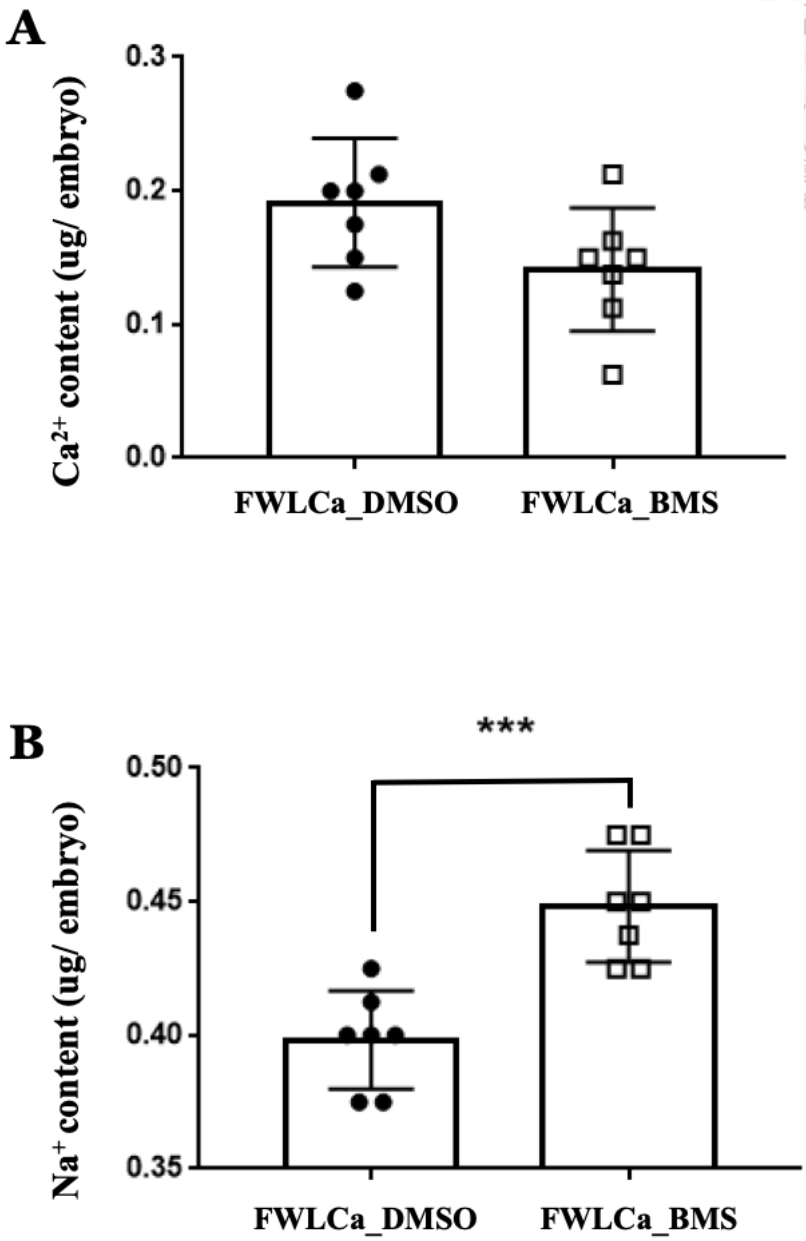

Fig 10. Contents of Ca^{2+} and Na^{+} in FWLCa acclimated embryos after BMS-754807 treatment. Contents of Ca^{2+} (A) and Na^{+} (B) in 6 dpf whole mount embryos were measured after 3 days of artificial FWLCa acclimation and 1 day BMS-754807 treatment before sampling. BMS-754807 did not affect the Ca^{2+} contents but significantly increased the content of Na^{+}. DMSO were added as vehicle control. Values are the mean ± SD (n=7). Student's *t*-test, ***$p < 0.001$.

doi:10.6342/NTU202002011

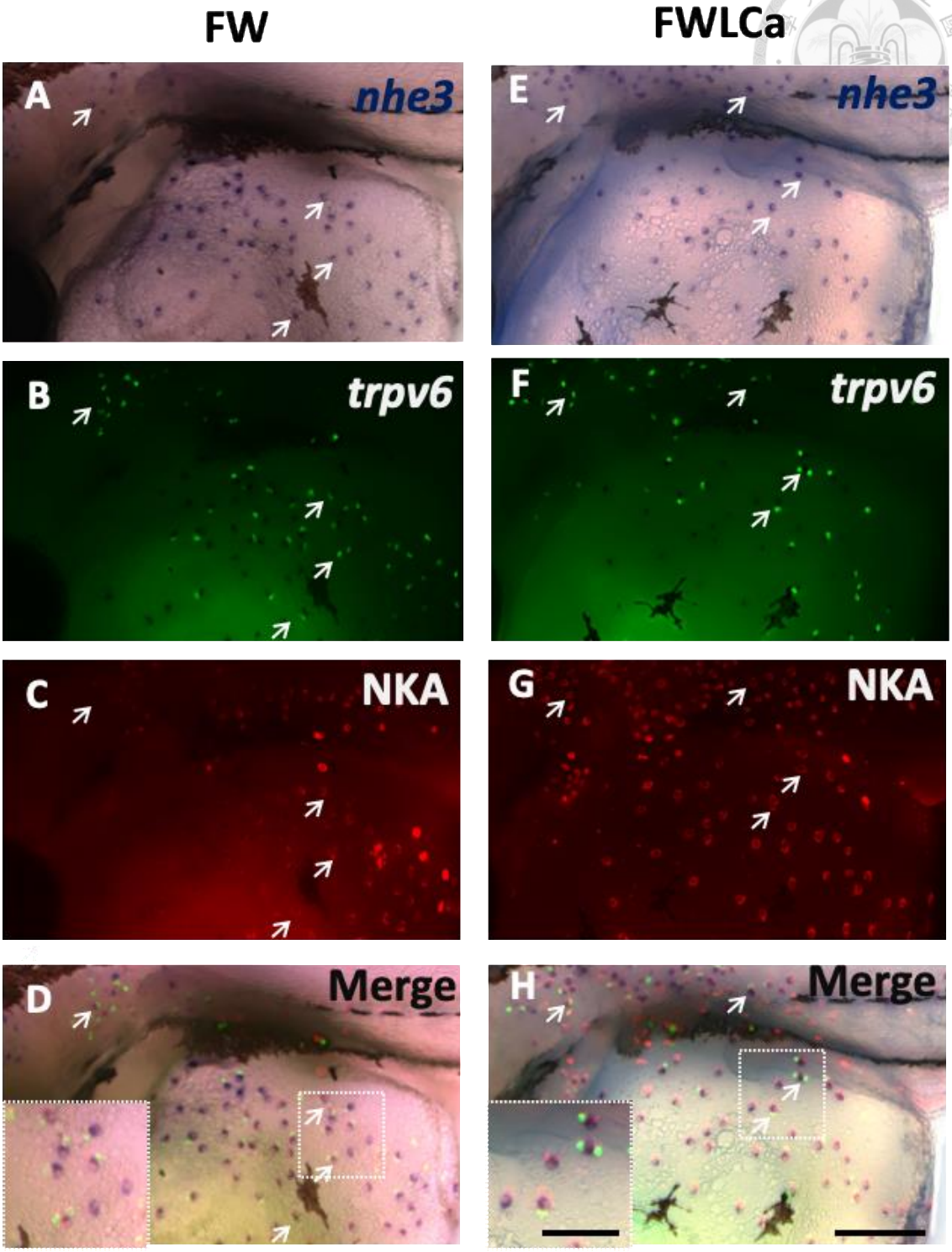

Fig. 11. Localization of *trpv6* and *nhe3* in FW/FWLCa acclimated medaka. The expression pattern of *nhe3* (A and E) and *trpv6* (B and F) were analyzed by double-labeled ISH in 3dpf medaka embryos transferred to FW (A-D) or FWLCa (E-H) until to 6 dpf.

doi:10.6342/NTU202002011

NKA immunostaining labeled ionocytes (C and G). Merged images of (A-C) and (E-G) were showed in (D) and (H), respectively. The expression of *nhe3* expressing cells is co-localized with NKA labeling ionocytes, and *trpv6* is expressed in the neighboring cells of *nhe3* expressing ionocytes. White arrow indicates a cluster of *trpv6* and *nhe3* expressing cells. Scale bar indicates 50 μm in the partial enlargements of the dotted frames, and 100 μm in A-H.

doi:10.6342/NTU202002011

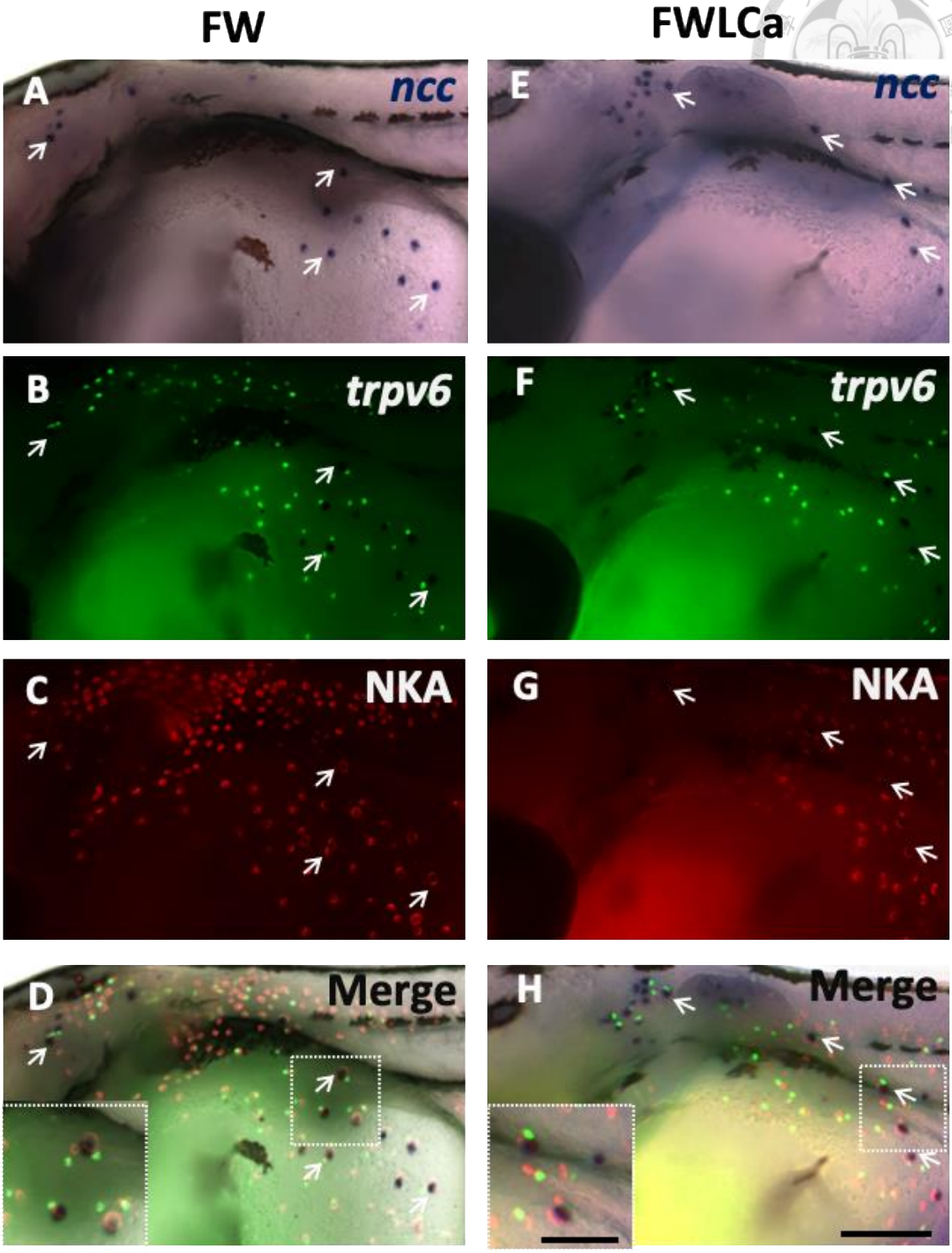

Fig. 12. Localization of *trpv6* and *ncc* in FW/FWLCa acclimated medaka. The expression pattern of *ncc* (A and E) and *trpv6* (B and F) were analyzed by double-labeled ISH in 3dpf medaka embryos transferred to FW (A-D) or FWLCa (E-H) until to 6 dpf.

doi:10.6342/NTU202002011

NKA immunostaining labeled ionocytes (C and G). Merged images of (A-C) and (E-G) were showed in (D) and (H), respectively. The expression of *ncc* expressing cells is co-localized with NKA labeling ionocytes. The number of *trpv6* expressing cells is much more than *ncc* expressing ionocytes, but almost all *ncc* expressing ionocytes does have *trpv6* expressing cells localize next to it. White arrow indicates *trpv6* and *ncc* expressing cells. Scale bar indicates 50 μm in the partial enlargements of the dotted frames, and 100 μm in A-H.

doi:10.6342/NTU202002011